Potential for shoreline recession to accelerate discharge of groundwater pollutants to coastal waters

Sabina Rakhimbekova[1], Christopher Power[1], Denis O'Carroll[2], and Clare Robinson[1]

[1]Western University
[2]University of New South Wales

December 22, 2022

Abstract

Discharge of groundwater-derived pollutants to inland and marine coastal waters is influenced by the transport and reactive processes occurring in nearshore aquifers. The effect of shoreline change on these processes and subsequent discharge of pollutants to coastal waters is unclear. The objective of this study was to evaluate the impact of shoreline recession (landward movement of the mean shoreline) on the transport of nitrogen [N] and phosphorus [P] in a nearshore aquifer and their discharge to coastal waters. Field investigations were conducted on a permeable unconfined nearshore aquifer on Lake Huron, Canada, in years coinciding with historically low and high lake water levels. At the site, a septic system-derived nutrient-rich (N and P) groundwater plume is moving towards the lake and the mean shoreline position moved ~30 m landward between sampling years due coastal erosion and mean lake water level increase. Data indicate PO4-P fluxes to the lake were higher following shoreline recession due to shortened travel pathways. In contrast, NO3-N fluxes were governed by the specific geochemical conditions near the sediment-water interface, which are not only a function of the shoreline position. Further, findings show shoreline recession may modify mineral phases that tend to sequester pollutants (e.g., iron oxides) near the sediment-water interface and this may possibly mediate release of sediment-bound pollutants. The findings provide new insights into potential impacts of shoreline change on chemical discharge to coastal waters as needed to inform long-term water quality predictions and management.

Potential for shoreline recession to accelerate discharge of groundwater pollutants to coastal waters

Sabina Rakhimbekova[a*], Christopher Power[a], Denis M. O'Carroll[b], Clare E. Robinson[a]

[a] Department of Civil and Environmental Engineering, Western University, London, ON, Canada.

email: srakhimb@uwo.ca

[b] School of Civil and Environmental Engineering, Water Research Laboratory, University of New South Wales, Manly Vale, NSW 2093, Australia.

*corresponding author: Dr. Sabina Rakhimbekova

Key points:

- Increase in inland coastal water level resulted in ~ 30 m shoreline recession
- Shoreline recession accelerated PO_4-P discharge due to reduced travel paths
- Geochemical conditions near the shoreline governed fate and discharge of NO_3-N
- Shoreline recession modified location of "iron curtain"

Abstract

Discharge of groundwater-derived pollutants to inland and marine coastal waters is influenced by the transport and reactive processes occurring in nearshore aquifers. The effect of shoreline change on these processes and subsequent discharge of pollutants to coastal waters is unclear. The objective of this study was to evaluate the impact of shoreline recession (landward movement of the mean shoreline) on the transport of nitrogen [N] and phosphorus [P] in a nearshore aquifer and their discharge to coastal waters. Field investigations were conducted on a permeable unconfined nearshore aquifer on Lake Huron, Canada, in years coinciding with historically low and high lake water levels. At the site, a septic system-derived nutrient-rich (N and P) groundwater plume is moving towards the lake and the mean shoreline position moved ~30 m landward between sampling years due coastal erosion and mean lake water level increase. Data indicate PO_4-P fluxes to the lake were higher following shoreline recession due to shortened travel pathways. In contrast, NO_3-N fluxes were governed by the specific geochemical conditions near the sediment-water interface, which are not only a function of the shoreline position. Further, findings show shoreline recession may modify mineral phases that tend to sequester pollutants (e.g., iron oxides) near the sediment-water interface and this may possibly mediate release of sediment-bound pollutants. The findings provide new insights into potential impacts of shoreline change on chemical discharge to coastal waters as needed to inform long-term water quality predictions and management.

Keywords: climate change, shoreline erosion, coastal water level change, nutrients, iron curtain, septic system

1 Introduction

Coastal zones are the most populated and developed areas worldwide. Currently over half of the global population resides in coastal areas and this is expected to increase in the future based on current trends of coastal migration and population growth (Small and Nicholls, 2003). Sandy beaches, which occur along marine coastlines and along inland coastlines that are adjacent to large inland lakes, make up more than one-third of the ice-free global coastline (Luijendijk et al., 2018). Many sandy coastlines worldwide are threatened by the landward movement of the shoreline, known as shoreline recession. Shoreline recession, which is caused by increases in coastal water levels (i.e. sea level rise or lake level changes) combined with shoreline erosion, is expected to increase as the climate changes (e.g., higher frequency and more intense storm events) and in response to anthropogenic development (Bird, 2008). Luijendijk et al. (2018) found from satellite image analysis that 24% of the world's sandy beaches are eroding at rates exceeding 0.5 m/yr, with only 48% of sandy beaches considered stable. For the Laurentian Great Lakes, which have more than 6000 km of permeable shoreline (Government of Canada - Environment and Climate Change Canada and U.S. EPA, 2009), shoreline recession caused by interannual lake water level fluctuations combined with erosive storm events is an increasing challenge. Lake water level fluctuations up to one to two meters occur along large lacustrine shorelines, such as the Great Lakes, approximately once a decade (Argyilan and Forman, 2003; Sellinger et al., 2008).

It is well established that shoreline recession along marine and inland coastlines has severe economic, social and environmental consequences due to impacts including land and habitat loss, property damage, and reduced revenue potential from tourism and industry

(Mukhopadhyay et al., 2018; Theuerkauf et al., 2019). As such, this is an active area of research, with studies generally focused on monitoring shoreline changes (e.g. Burningham and French, 2017; García-Rubio et al., 2015; Hagenaars et al., 2018), fundamental understanding of underlying geomorphological and hydrological processes (e.g. Brooks et al., 2017; Swenson et al., 2006), and techniques for forecasting shoreline change over short and long time scales (e.g. Davidson et al., 2017; Mukhopadhyay et al., 2018). Few studies have examined the potential impacts of shoreline recession, including sediment erosion and changes in coastal water levels, on the flux of land-derived pollutants to coastal waters. Two prior studies examined on the impact of shoreline erosion on nutrient loading to Lake Tahoe, United States (Adams and Minor, 2002) and Lake Diefenbaker Reservoir, Canada (Hewlett et al., 2015). Both studies found that nutrient loading caused by shoreline erosion (due to release of sediment-bound nutrients) only contributed a fraction of the total nutrient load into the lakes (< 5% of total nutrient input). More recently, beach sand erosion was found to be the main mechanism of transferring *E.coli* to nearshore coastal waters during intensified wave conditions at a sandy beaches (Vogel et al., 2016). Finally, focused on a coastal wetlands rather than sandy shorelines, Braun et al. (2019) showed that shoreline recession may reduce the carbon storage potential of a coastal wetland and thereby impact carbon dynamics within the wetland. The above-mentioned studies all focus on sediment-bound pollutants that are released to coastal waters as sediment near the shoreline is eroded and released to the coastal waters. While this can be an important transport mechanism, shoreline recession may also affect the delivery of dissolved pollutants into coastal waters, particularly land-derived groundwater pollutants, whose delivery to coastal waters strongly depends on the specific subsurface transport pathways between the land source and coastal

waters, as well as the geochemical conditions along these pathways in nearshore aquifers (Bełdowska et al., 2022; Destouni et al., 2010). For instance, shoreline recession brings the shoreline closer to areas of human development (e.g. infrastructure, landfills, and contaminated sites), which decreases the distance between a groundwater pollution source and the coastal water. This may in turn increase the potential for groundwater-derived pollutants reaching coastal waters.

Submarine groundwater discharge (SGD) and lacustrine groundwater discharge (LGD) are important pathways for land-derived pollutants such as nutrients, metals and organic contaminants to enter marine and inland coastal waters, respectively (e.g. Beck et al., 2016; Lewandowski et al., 2015; Moore, 2010). With increased urbanization, industrialization and intensification of agriculture in coastal areas, groundwater pollutant concentrations can be high in coastal areas and pose a risk to coastal water pollution. The importance of LGD has mainly been recognized for its contribution to lake nutrient loads and lake eutrophication (Robinson, 2015; Rosenberry et al., 2015). For instance, high nutrient concentrations, more than ten times higher than in the adjacent lake water, were observed in groundwater discharging into Lake Simcoe (Roy and Malenica, 2013). In addition to nutrients, studies have also shown that LGD may play an important role in delivering other chemical constituents, including metals (Lee et al., 2014; Rakhimbekova et al., 2018) and road salt (Howard and Livingstone, 2000; Roy, 2019) to lakes. The transport of pollutants via groundwater flow paths to coastal waters is generally slow, and transport can be retarded by various physical and chemical processes (e.g. filtration, sorption, precipitation). Therefore, changes in the shoreline position may impact the groundwater travel times, travel distances and the specific pathways, by which pollutant are transported

from their land source to coastal waters. In addition, it is well established that an important reaction zone can exist in nearshore aquifers close to the shoreline due to the mixing of groundwater and coastal water. This zone, commonly referred to as a subterranean estuary in marine environments, is known to strongly influence the discharge of groundwater-derived pollutants to coastal waters due to its high reactivity (Rakhimbekova et al., 2021b, 2021c; Robinson et al., 2018). One important reactive phenomenon in this mixing zone is the sequestration (trapping) of pollutants to sediment mineral phases, particularly iron (Fe) oxides, which form under certain redox and pH conditions. This sediment trap mechanism, commonly referred to as the "iron curtain", can act as a natural barrier that limits the release of a range of pollutants, including phosphorus (Charette and Sholkovitz, 2002; Spiteri et al., 2008), carbon (Linkhorst et al., 2017; Sirois et al., 2018), metals (McAllister et al., 2015), and trace metals (Beck et al., 2008) to coastal waters. It is possible shoreline recession may cause a shift in the location of the mixing zone, thereby impacting reactivity and geochemical conditions, including the function of sediment trap and its ability to sequester pollutants. This may in turn modify pollutant fluxes delivered to coastal waters via SGD and LGD.

To the best of our knowledge, there are no studies that have explored the impact of shoreline changes, including shoreline recession, on the discharge of groundwater-derived pollutants to coastal waters. The objective of this study is to address this knowledge gap. Field data collected downgradient of a large septic system over a six-year period is used to examine the influence of shoreline recession on the subsurface transport of a P- and N-rich wastewater plume and its potential discharge to the adjacent lake. In addition, the study investigates the way in which shoreline recession may alter geochemical conditions near

the sediment-water interface with a specific focus on the abundance and distribution of mineral phases that tend to sequester pollutants, including P, close to the groundwater-coastal water interface. Finally, this study explores the broader possible impacts of shoreline recession beyond our specific study site by discussion of potential sources of anthropogenic groundwater contaminant sources along shorelines and future projections on lake water level changes and expected shoreline changes. The findings of this study are needed given the prevalence of groundwater contamination near marine and inland coastlines, and the projected changes in coastal water levels and storm intensity and frequency as the climate changes.

2 Methodology

2.1 Field investigation

2.1.1 Site description

Field investigations were conducted at Ipperwash Beach on Lake Huron, Ontario, Canada in 2014, 2015, and 2020 (Figure 1a). Ipperwash Beach is a sandy beach that extends over 20 km and has an extensive dune system behind the beach that rises several meters above the lake surface (Eyles and Meulendyk, 2012). Extensive shoreline recession occurred at Ipperwash Beach between 2015 and 2020 in response to an increase in the water level in Lake Huron combined with beach erosion. In 2020, the water level in Lake Huron reached 177.45 m (IGLD 85 datum) following over a decade of low water levels during which the record low water level of 175.57 m occurred in 2013 (Gronewold et al., 2021; Gronewold and Stow, 2014). The extent of shoreline recession between 2015 and 2020 are illustrated in aerial photographs shown in Figure 1b.

Ipperwash Beach was selected for this study as a public comfort station with a large septic system is located in close vicinity to the beach (Figure 1b). The septic system has been operational since at least 1974 and is only used during the warmer months from May to September. Due to shoreline recession, the mean shoreline position was located ~120 m from the septic system tile bed in 2015, but only ~90 m from the septic tile bed in 2020 (Figure 1b). Detailed (approximately monthly) field sampling was conducted between August and October in 2014, and between May and August in 2015, to evaluate the spatial and temporal variability of phosphorus (P) and nitrogen (N) transport from the septic system through the nearshore aquifer to the lake. Details of this previous study are provided in Rakhimbekova et al. (2021a). This current study expands upon this prior work with new sampling performed in 2020 to determine the impact of shoreline recession on the transport of P and N through the nearshore aquifer and their potential discharge to the lake.

2.1.2 *Field monitoring approach*

2.1.2.1 *Field equipment*

For all sampling periods in 2014-2015 and 2020, a cross-shore monitoring transect was installed that aligned with the center of the septic system-derived nutrient-rich plume that is moving towards the lake. The original cross-shore monitoring transect in 2014-2015 consisted of ten multi-level samplers (MLS) and extended from ~71 m downgradient of the septic tile bed (x = 71 m; landward extent of the beach dunes) to ~20 m offshore (x = 140 m; Figure 1c). For the 2020 sampling, the cross-shore monitoring transect consisted of six MLS, and extended from x = 71 m downgradient of septic tile bed ~20 m offshore (x = 110 m) (Figure 1c). The x-z coordinate system used herein is defined with x = 0 m located at the landward edge of the septic tile bed and z = 0 as the elevation of a local permanent

benchmark. All MLS were installed up to 3 m below ground surface, with sampling ports at 0.2 m depth intervals.

Two piezometers (PZ) were permanently installed at x = 71 m (PZ-1) and x = 93 m (PZ-2) in July 2014, with additional piezometers temporarily installed along the cross-shore monitoring transect at the start of each sampling event to measure the groundwater and lake water levels across the nearshore aquifer and offshore. The location of monitoring equipment and ground surface elevations were surveyed with a total station (Topcon GTS-239W) relative to a local permanent benchmark during each sampling event (Figure 1c).

2.1.2.2 *Electrical resistivity imaging*

The septic system origin of the nutrient-rich plume observed in the nearshore aquifer was confirmed in 2015 by using artificial sweeteners as a chemical tracer for human wastewater (Rakhimbekova et al., 2021a). However, the artificial sweetener data were limited to point information obtained from samples collected at selected MLS located over 70 m downgradient of the septic tile bed (i.e., samples collected from x = 71 m onwards). During the field sampling in 2020, a non-invasive electrical resistivity tomography (ERT) survey was performed to provide continuous imaging of electrical resistivity within the subsurface and determine if this approach would be able to trace the nutrient-rich plume back to the septic tile beds.

An ERT survey line consisting of 96 stainless-steel electrodes (0.3 m) with an inline spacing of 1 m was deployed. The location of the line coincided with the location of the cross-shore monitoring transect but it extended from the landward edge of the septic tile bed (x = 0 m) to the shoreline (x = 95 m) (Figure 1b). A multi-channel Syscal Pro Switch

48 resistivity system (IRIS Instruments, France) was used to complete the survey. As this system is limited to 48 electrodes at a time, the roll-along method was used to record the survey line through three successive segments. For this, 24 electrodes were moved for each segment to ensure 50% overlap (i.e., electrode numbers: 0-48, 24-72, 48-96) (Robinson et al., 2022).

The multi-gradient electrode array was used with a total of 4183 measurements. Due to the dry surface sand, saline water was added around each electrode to ensure strong ground coupling (resistance: <1 kilo-ohm). The recorded apparent resistivity data was inverted with DC_2DPro, an iterative least-squares smoothness-constrained inversion program (Kim, 2016). The surface elevation at each electrode, which was surveyed using the total station, was incorporated into the inversion, which was then run to a maximum of seven iterations, showing good convergence with a low root mean square (RMS) error of 5.5%.

2.1.2.3 *Porewater sampling and analysis*

For all sampling events, pore water samples were first collected from all MLS ports using syringes attached to the PVC sampling tubes (ϕ = 1.35 mm). Porewater samples were collected from each port, filtered using 0.45 µm cellulose acetate filters, and stored in 60 mL HDPE bottles. Samples were analyzed for phosphate (PO_4-P), nitrate (NO_3-N) and chloride (Cl) within 48 hours of collection. After samples were collected, a peristaltic pump was used to draw pore water directly into a flow cell where pH, electrical conductivity (EC) and temperature were measured with an In-Situ Multi-Parameter TROLL® 9500 and YSI 6600 V2 Sonde. Multiple nearshore lake water samples were also collected during each sampling event. Collected pore water samples were analyzed for nutrients (PO_4-P, NO_3-N)

using Lachat 750 Flow Injection Analysis (Lachat 750), and Cl using High Performance Liquid Chromatography.

2.1.2.4 *Sediment sampling and analysis*

During MLS installation in May 2015 and August 2020, multiple sediment samples were collected at depths of 0.5 m to 2 m below the ground surface for sediment chemistry characterization (Figure 1c). Sediment samples were analyzed via total acid digestion using method EPA 200.8 (US EPA, 1996) to determine the total elemental solid phase concentrations. In addition, due to the potential importance of Fe-bearing solid phases in sequestering chemical including P in nearshore aquifers, select sediment samples were treated with (i) acid ammonium oxalate solution (McKeague and Day, 1966), and (ii) dithionite-citrate-bicarbonate solution (Mehra, 1958) to provide characterization of the Fe-bearing solid phases (e.g. degree of crystallization). Oxalate-extractable Fe (Fe_o) is operationally thought to represent amorphous oxides such as ferrihydrite and small amounts of organically-bound Fe (Schwertmann, 1964). Dithionite-extractable Fe (Fe_d) is operationally thought to represent organically-bound oxides, amorphous oxides, and finely crystalline oxides (Akinbola et al., 2013). The difference between Fe_d and Fe_o generally represents the amount of solid phase Fe present in crystalline oxide forms (e.g., goethite and hematite). Total dissolved phosphorus (TDP) and total iron (Fe) in extractant solutions were analyzed using HACH DR 6000 UV VIS Spectrophotometer and inductively-coupled plasma mass spectroscopy (ICP-MS), respectively. Additional details on sediment sample analysis are provided in the Supporting Information (SI Section 1).

2.2 Numerical model

A two-dimensional (2D) model was developed in MODFLOW-NWT (Niswonger et al., 2011) to simulate steady state groundwater flows and estimate NO_3-N and PO_4-P loads discharging to the lake along the vertical cross-shore section. The model domain and parameterization were based on a groundwater model of the study site developed and validated by Malott et al. (2016). The two-dimensional model assumes negligible groundwater flow in the alongshore direction. The model was 150 m long in the cross-shore direction and the aquifer thickness at the shoreline location was set to 13 m at the landward boundary due to presence of a clay layer at this depth according to local well records (Figure 2). The beach face and lake boundaries (AB and BC) were specified based on topographic sand level surveys conducted during each sampling period. The model was discretized into 71 layers and 128 columns with greater refinement around the shoreline and the beach face. Grid discretization tests were performed to ensure a converged solution. Particle size analysis performed on sediment samples (n = 7) collected across the nearshore aquifer up to 2.5 m below the water table indicated that the nearshore aquifer is comprised of relatively homogeneous fine sand (Coefficient of Uniformity, C_u = 2.18 and sand grain size, d_{50} = 0.16 mm) with the saturated K estimated to range from 7 to 15 m/d using the method of Krumbein and Monk (1943). Based on this, the simulated aquifer was homogeneous and isotropic with the hydraulic conductivity (K) set to 10 m/d and effective porosity n = 0.3.

The upper (AB) and bottom (ED) model boundaries were no-flow boundaries assuming negligible aerial recharge and evaporation, and an impermeable aquifer basement, respectively. The offshore boundary (CD) was specified as no-flow boundary and was

located sufficiently far from the shoreline (>50 m offshore) that it did not influence the groundwater flows in the nearshore aquifer (Figure 2). The vertical landward boundary (AE) was located at x = 60 m, which is 10 m inland from the landward extent of the beach dunes (Figure 2) and was set to be a constant head boundary. Three simulations were run with the boundary conditions modified to represent the mean hydrological conditions at the study site during the 2014, 2015 and 2020 sampling periods. Based on the measured groundwater levels, the hydraulic head at the landward boundary was set to -2.95 m, -3.05 m and -1.95 m, respectively, for the models simulating the groundwater flows over the sampling periods in 2014, 2015 and 2020. A constant head condition was used along the lake boundary (BC) with the specified head values set based on the mean measured lake water level during each of the sampling periods and considering the effect of steady waves acting on the boundary. To simulate the effect of steady waves, the approach of Anwar et al. (2014) was adopted whereby the time-averaged effect of waves as described by wave set-up was used (details are provided in SI Section 2). For this, the empirical equation of Nielsen (2009) was used to estimate the wave-set up profile and calculate head values that were then prescribed along the lake boundary (BC). Offshore root mean square wave heights (H_{rms}) of 0.35 m, 0.25 m and 0.35 m were used in the equation of Nielsen (2009) to simulate the mean wave conditions over the sampling periods in 2014, 2015 and 2020, respectively. The mean H_{rms} values were calculated using monitoring data from a wave buoy located ~35 km from the study site (C45149 Southern Lake Huron, Department of Fisheries and Oceans Canada Buoy, 2020). Based on the mean lake water levels measured at the study site during the sampling periods in 2014, 2015 and 2020, the still lake water level in the models were set to -3.64 m, -3.73 m and -2.21 m, respectively.

3 Results and discussion

3.1 Field and modeling results

3.1.1 Change in hydrological conditions between sampling periods

The hydrological conditions at the study site including the mean lake water level, mean wave conditions, and landward groundwater levels varied between the sampling periods. The mean lake water level was approximately 0.7 m higher in 2020 compared to 2014-2015 (Figure 3a). More intensified wave conditions were also observed in 2020 compared to 2014-2015 with maximum wave height (H_{rms}) reaching 3.7 m in 2020 compared to 3.0 m in 2014 and 2.1 m in 2015 (mean H_{rms} was 0.35 m, 0.25 m and 0.35 m in 2020, 2015 and 2014, respectively; Figure 3b). The extent of shoreline recession between 2015 and 2020 is evident by comparing the topographical surveys performed in 2015 and 2020, along with corresponding aerial photographs (Figures 1b and 1c). The shoreline was estimated to move 30 m landward from x = 120-125 m in 2014-2015, to x = 90 m in 2020, in response to the lake water level increase and beach sand erosion.

Increase in lake water levels may lead to a corresponding increase in the landward groundwater table elevation, and thereby reduce the vertical separation between septic tile beds and groundwater table. This can be a concern as it then limits the efficiency of the septic tile bed in attenuating wastewater constituents including nutrients (Mitchell et al., 2021). Based on groundwater levels measured at PZ-1 (x = 71 m), there was ~ 1 m increase in the groundwater table between 2014-2015 and 2020 (Figure 1c). However, with high sand dunes behind the beach, there is a thick (3 - 4 m) vadose zone below the septic tile beds at this study site (see Section 3.1.2 for details), and therefore it is not expected that the higher groundwater table elevation in 2020 compared to 2014 – 2015 would have

adversely impacted the function of the vadose zone below the septic tile beds in attenuating wastewater constituents. The adverse impact of increasing coastal levels on the attenuation of wastewater constituents below the septic tile beds is expected to be a larger concern in coastal plain settings with flatter topography and shallow groundwater tables.

The mean hydraulic gradient across nearshore aquifer was negative in 2014-2015 (h = -0.015) and 2020 (h = -0.017), indicating lakeward groundwater flow. Based on the hydraulic gradient in 2014-2015 and 2020, mean hydraulic conductivity (K = 10 m/d) and effective porosity (n = 0.3) for the nearshore aquifer, the mean horizontal groundwater velocity towards the lake is estimated to be 0.50 m/d in 2014-2015 and 0.56 m/d in 2020. Numerical simulations show the change in groundwater flow patterns (Figure 4a-c) in the nearshore aquifer between the 2014-2015 and 2020 sampling periods with the groundwater discharge zone shifting from x = 120-125 m in 2014-2015 to x = 85-90 m in 2020. Based on the estimated overall mean horizontal velocities and shoreline positions, the travel time for conservative species to be transported from the septic tile bed to the shoreline is estimated to be around 240 days in 2014-2015 compared to only 160 days in 2020.

While the flow patterns simulated by the steady state groundwater models do not indicate recirculation of lake water through the nearshore aquifer (Figure 4a-c), recirculating flows driven mostly by changing lake water levels and wave conditions are expected to occur landward of the mean shoreline position and simulated groundwater discharge zone (Malott et al., 2016). With the mean shoreline position and zone of groundwater discharge shifting landward in 2020 compared to 2014-2015, the recirculation zone, which is generally associated with high reactivity including the presence of mineral phases (e.g., Fe oxides) that tend sequester pollutants (Lee et al., 2014; Lewandowski et al., 2015; Rakhimbekova

et al., 2018), would also have shifted landward. It is possible that this landward shift in the recirculation zone could have altered geochemical conditions in the nearshore aquifer and this is explored in the following sections.

3.1.2 Characterization of septic-derived nutrient plume

Elevated groundwater PO_4-P and NO_3–N concentrations were observed at the study site in 2014, 2015 and 2020 (Figures 4d to 4i). Groundwater PO_4-P concentrations ranged from 8 to 166 μg/L in 2014-2015, and from 3 to 98 μg/L in 2020. Maximum PO_4-P concentrations in the nearshore aquifer exceeded the upper limit of the Canadian Water Quality Guidelines for the Protection of Aquatic Life for Total Phosphorus to limit eutrophic conditions (35–100 μg P/L; Canadian Council of Ministers of the Environment, 2014), and were considerably higher than the mean measured lake water concentrations for all sampling periods (2-3 μg/L). Groundwater NO_3–N concentrations ranged from 4 to 57 mg/L in 2014-2015 and from 1 to 26 mg/L in 2020. Maximum NO_3-N concentrations in the nearshore aquifer exceeded the Canadian Water Quality Guidelines for the Protection of Aquatic Life for all sampling periods (3 mg/L; Canadian Council of Ministers of the Environment, 2014), and were also higher than the mean measured lake water concentrations (0.2-0.8 mg/L).

Figures 4j-l to 4m-o presents the distributions of chloride (Cl) concentrations and electrical conductivity (EC) measured along the monitoring transect in 2014, 2015 and 2020. Cl and EC can be considered conservative wastewater tracers at the site(Rakhimbekova et al., 2021a), and their distributions generally coincide with the locations of elevated PO_4-P and NO_3–N in the nearshore aquifer Figure 4d-i. NO_3–N with EC landward of the maximum shoreline position are correlated (Figure S1) indicating the suitability of using ERT for

characterizing the spatial extent of the high nutrient groundwater plume. Figure 5 shows a 2D cross-sectional ERT image that extends from x = 0 m (septic tile bed) to x = 95 m (near the mean shoreline position in 2020). The location of the septic tile bed, PZ-1 and MLS are indicated in the figure, along with the lake water and groundwater levels measured during the survey. The highly resistive near surface layer between x = 0 m and x = 78 m (red-purple; >1000 ohm-m) represents the vadose zone with a mean thickness of approximately 4 m. The underlying layer of low resistivity (blue-green; <150 ohm-m) represents the zone of saturated groundwater, with some areas having very low resistivity (<50 ohm-m). The ERT image can be validated by comparing bulk resistivity values with the porewater EC measurements in Figure 4m-o. For example, the porewater EC at x = 71 m and z = -3 m (PZ-1) is 1008 μS/cm which suggests a bulk EC of 209 μS/cm, or bulk resistivity of 48 ohm-m (Archie, 1942) – this closely matches the bulk resistivity inferred by ERT at that location (55 ohm-m). Figure 5 indicates that the zone of very low bulk resistivity is connected to the base of the septic tile bed and extends lakeward. This zone exists through the shallow nearshore aquifer and becomes shallower near the shoreline meeting the sediment-water interface around x = 92 m. This ERT image clearly illustrates that the elevated NO_3-N and PO_4-P concentrations observed near the shoreline originate from the septic tile bed.

3.1.3 Impact of shoreline recession on PO_4-P

As seen in Figure 4, the highest PO_4-P concentrations were observed 73-90 m lakeward of the septic tile bed (maximum PO_4-P = 166 μg/L; x = 73-90 m) in 2014-2015, with concentrations decreasing closer to the shoreline (particularly in 2015). However, elevated concentrations of the conservative wastewater tracers, Cl and EC, near the shoreline (x =

115-125 m) for these sampling periods suggest that the septic-derived wastewater plume has reached the shoreline. Taking into account septic system operation time, groundwater velocity, and length of the PO_4-P plume in 2015, Rakhimbekova et al. (2021) concluded that PO_4-P transport in the nearshore aquifer was mainly governed by retardation. Based on the location of the PO_4-P plume in 2015, it was predicted that PO_4-P may possibly reach the shoreline in approximately 10 years. However, this prediction is incorrect due to shoreline recession at the site. Figure 4f shows that in 2020 (within <5 years), the PO_4-P plume has reached the new shoreline location (x = 90 m). To provide a quantitative estimate on the extent to which PO_4-P fluxes to the lake may have changed, the measured PO_4-P concentrations were combined with the simulated groundwater flows for each sampling period. PO_4-P fluxes were calculated by multiplying PO_4-P concentrations (interpolated to a depth of 3 m below ground surface) along vertical line near the shoreline (x = 120.3 m in 2014 and 2015 and x = 88.7 m in 2020; Figure 4 a-c) by simulated groundwater fluxes directed towards the lake for each sampling year (Additional details provided in SM S3). From these calculations, it is estimated that the PO_4-P flux to the lake may have increased nearly tenfold from 53 mg/d/m in 2015 to 482 mg/d/m in 2020 (Figure 6a) due higher PO_4-P concentrations near the shoreline in 2020 compared to near the shoreline in 2015 as well as slightly higher lakeward-directed groundwater velocity (Figure 4e, f). This result illustrates that the shoreline recession can accelerate the discharge of groundwater-derived pollutants that are slowly advancing towards the shoreline by decreasing the subsurface travel distance and time.

3.1.4 Impact of shoreline recession on NO_3-N

The NO_3-N distribution in the nearshore aquifer was influenced by not only its shorter discharge pathway through the nearshore aquifer due to shoreline recession but also by the specific geochemical conditions near the sediment-water interface that impact reactive transformations that NO_3-N may undergo prior to its discharge. Rakhimbekova et al. (2021a) previously showed that the extent of NO_3-N removal that occurs in the nearshore aquifer prior to discharge may vary over time as the extent of denitrification changes in response to changing geochemical conditions near the sediment-water interface (e.g., due to changes in organic matter availability). Rakhimbekova et al. (2021a) presented detailed data analysis showing changing organic matter availability was associated with the observed decrease in NO_3–N concentrations near the shoreline in 2015 (0-2 mg/L) compared to 2014 (4-67 mg/L), and thus lower estimated NO_3-N flux towards the lake in 2015 (4 mg/d/m) compared to 2014 (124 mg/d/m) (Figure 6b).

NO_3–N concentrations observed near the mean shoreline position in 2020 (x = 85-90 m) ranged from 4 to 26 mg/L in 2020 (Figure 4i). The estimated NO_3-N flux directed towards the lake near the shoreline in 2020 (79 mg/d/m) was larger than in 2015 (4 mg/d/m) but smaller than in 2014 (124 mg/d/m). NO_3-N flux is affected by both groundwater velocity and NO_3-N concentrations. Since groundwater velocity near the shoreline was slightly higher in 2020 compared to 2014 (difference in flow arrow sizes in Figure 4 a-c), the higher estimated NO_3-N flux in 2014 is due to higher NO_3-N concentrations near the shoreline in 2014 compared to 2020. Therefore, even though shoreline recession reduced the travel distance and travel time for the septic-derived NO_3-N to reach the lake, the specific geochemical conditions in the nearshore aquifer near the shoreline ultimately govern the

flux of NO_3-N to the lake rather than the overall travel distance and time. This finding is in contrast to the highly retarded PO_4-P plume for which shoreline recession was found to directly accelerate PO_4-P discharge to the lake due to the overall reduced travel distance between the septic tile bed and shoreline.

It is important to note that while the geochemical conditions near the shoreline have a controlling influence on the fate of NO_3-N in the nearshore aquifer and its flux to the lake at our study site, this may not be the case at other sites. The nearshore aquifer at our study site (from the septic tile bed to shoreline) is predominantly oxic and therefore limited denitrification occurs as NO_3-N is transported towards the shoreline. At other sites where the nearshore aquifer is more reducing, it is possible that the decrease in overall travel distance and times could limit the extent of denitrification that occurs as NO_3-N is transported from the source to the coastal water (Meile et al., 2010). Further, it is possible that shoreline recession could have a greater impact on the discharge of reactive pollutants in nearshore aquifers with sharper geochemical (redox and pH) gradients than observed at Ipperwash Beach (Rakhimbekova et al., 2021a, 2018).

3.1.5 Impact of shoreline recession on Fe curtain processes

In addition to modifying the physical transport pathways and travel times for the septic-derived nutrients being transported towards to the lake, the change in shoreline location may also modify the geochemical conditions near the groundwater-lake interface. In particular, it may modify the distribution, abundance and reactivity of mineral phases that can sequester pollutants in the nearshore aquifer. Rakhimbekova et al. (2021b) showed elevated solid phase Fe and P exists in the nearshore aquifer at the study site and suggested that PO_4-P derived from the decomposition of lake-derived organic matter may be

accumulating on Fe oxide minerals that exist close to the sediment-water interface. Previous studies in marine environments have similarly found that Fe oxides that form near the sediment-water interface can act as a geochemical barrier (i.e. “iron curtain”) with these minerals sequestering pollutants such as PO_4-P and limiting their release to coastal waters(Charette and Sholkovitz, 2002; Spiteri et al., 2006). While it is thought that sequestered pollutants may later be re-mobilized if geochemical or hydrological conditions change (Nisbeth et al., 2019; Spiteri et al., 2006), in this section we examine how the distribution and abundance of solid phase P and Fe, including Fe oxides, in the nearshore aquifer may have changed in response to shoreline recession.

Rakhimbekova et al. (201b) previously showed that nearshore aquifer at the study site is predominantly oxidizing, and there is no distinct redox gradient near the sediment-water interface. Further, Fe oxides are available through the nearshore aquifer and tend to accumulate PO_4-P on their mineral surfaces. Characterization of the distribution of solid phase P and Fe in the nearshore aquifer at the study site in 2015 and 2020 indicate a decrease in solid phase P and Fe between these times (Figure 7a-d). Due to the landward movement of the shoreline, sediment samples were taken in different locations in 2015 compared with 2020. To enable comparison of P and Fe solid phase concentrations between two times, comparison only considers samples collected over the same area, between x = 87 and 117 m (marked with red square on Figure 7). Generally, there was higher abundance of solid phase P near the shoreline in 2015 compared to 2020 (151 ± 51 μg/g in 2015, n = 17; 82 ± 55 μg/g in 2020, n = 23; Figure 7a and b). Solid phase Fe was also slightly higher in 2015 compared to 2020 (3.1 ± 0.6 mg/g in 2015, n = 17; 2.7 ± 0.7 mg/g in 2020, n = 23; Figure 7c and d).

Selective solid phase extractions were conducted to characterize Fe-bearing solid phases (amorphous, Fe_o and more crystalline, Fe_d) at the study site in 2015 and 2020. Again, only sediment samples collected between x = 87 and 117 m were used to compare the distribution of amorphous and crystalline Fe phases in 2015 and 2020. The abundance of Fe_o decreased between 2015 and 2020 (0.5 ± 0.2 mg/g in 2015, n = 10; 0.2 ± 0.09 mg/g in 2020, n = 13; Figure 7e and f). In contrast, Fe_d was slightly higher in 2020 compared to 2015 (0.5 ± 0.07 mg/g in 2015; 0.7 mg/g ± 0.3 in 2020; Figure 7g vs 7h). Lower Fe_d in 2015 compared to 2020 may possibly be due to the formation of more crystalline Fe phases over time. Larger difference in the abundance of Fe_o compared to Fe_d between 2015 and 2020 suggest that shoreline recession may have larger impact on amorphous Fe oxides compared to crystalline Fe oxides. This is not unexpected given that amorphous Fe oxides are less stable and shoreline recession may have altered factors that affect Fe oxide stability (e.g. oxygen availability, presence of bacteria) (Charette and Sholkovitz, 2002; Dean et al., 2003). Following shoreline recession, particularly a large erosive event, it might take time for amorphous Fe oxides to reform around the new shoreline location. This may explain the lower Fe_o near the new shoreline location in 2020 compared to higher Fe_o near the location of shoreline in 2015, which was a more stable shoreline position over the preceding years.

Amorphous Fe (e.g. ferrihydrite) tend to have a higher surface area that is more reactive and therefore has a higher capacity to sequester pollutants, including PO_4-P, compared to more crystalline Fe oxides fractions such as goethite and hematite (Fuller et al., 1993). Therefore, lower abundance of Fe_o in the nearshore aquifer in 2020 (following the shoreline recession) suggests that mineral surfaces along the groundwater discharge pathway may

have less ability to sequester PO_4-P, and this may possibily lead to higher PO_4-P fluxes to lake. The impact of shoreline recession on the distribution and abundance of Fe oxide minerals, particularly amorphous Fe oxides, is important as it may affect the function of these minerals in sequestering and releasing pollutants thereby modifying pollutant fluxes to coastal waters.

3.2 Broader implications of the impact of shoreline recession

The study findings demonstrate the potential impacts of shoreline recession driven by coastal water level changes and/or erosion on the transport and fate of groundwater pollutants and their discharge to adjacent coastal waters. The findings show shoreline recession may impact pollutants moving slowly along groundwater pathways towards the coastal water, as well as pollutants for which their fate and ultimate delivery to coastal waters is governed strongly by the geochemical conditions in the reaction zone that exists near the groundwater-coastal water interface. This section explores the broader implications of the study findings on the discharge of groundwater pollutants to the Laurentian Great Lakes, as well as other inland and marine coastal waters.

While it is known that water levels in the Great Lakes vary over 20 – 30 year cycles (Gronewold and Rood, 2019), recent future projections estimate that by 2040-2049 average annual water levels of Lake Superior, Lake Michigan-Huron and Lake Erie are projected to increase by +0.19, +0.44, +0.28 m, respectively due to an increase in over-lake precipitation and basin runoff compared to relatively smaller increase in lake evaporation (Kayastha et al., 2022). While there are no studies predicting future erosion rates and shoreline recession in response to the projected water level changes for the Great Lakes, several studies show that high water levels correspond with accelerated shoreline erosion,

including bluff erosion, on short time scales (e.g. Kaczmarek et al., 2016; Krueger et al., 2020). For instance, Castedo et al. (2013) simulated erosion rates to range between 0.5-1.5 m/yr in response to lake water level variations of 0.5-1 m. A more recent study by Volpano et al. (2020) on coastal bluff erosion along Western Lake Michigan's shoreline found that erosion rates increased from 0.18-0.43 m/yr between 2009 and 2014 (period with below long term average water levels) to 0.49-1.19 m/yr between 2014 and 2018 (period with above long-term average water levels).

The outlook for marine shorelines is also concerning. On average, global sea level has risen at a rate of 3-4 mm/yr in the last 20 years (Yi et al., 2015). Future projections estimate sea level rise from 0.1-0.2 m by 2050 and from 0.3-2 m by 2100 due to ocean warming and land-based ice melt (Kopp et al., 2014; Vitousek et al., 2017). While shoreline recession is generally the combined result of various contributing factors and may be complicated by local and regional differences, it is widely acknowledged that increasing sea levels will promote shoreline recession (e.g. Anderson et al., 2015; Bruun, 1962; Dean and Houston, 2016). For instance, a recent study predicted that 15% of world's sandy beaches could face severe coastal erosion by 2050 and up to 50% by the end of the century (Vousdoukas et al., 2020). Taking into consideration the projected sea level changes and associated shoreline recession, together with the findings of our study, there is high potential that future shoreline recession will modify inputs of groundwater pollutants to coastal waters.

While this study focuses on the wastewater plume from one septic system, there are 1.2 and 1.3 million septic systems in Ontario, Canada (DeRabbie, 2020) and Michigan, United States (Department of Environment, Great Lakes and Energy, 2022), respectively, with many of these septic systems located in close proximity to the shorelines of the Great Lake.

It is also important to note that in addition to nutrients, septic-derived wastewater effluent also contains other pollutants of concern including pharmaceuticals, personal care products and pathogens, all of which may pose a risk to coastal water pollution with associated human health and ecosystem impacts. Further, many other groundwater contaminant sources are often located in coastal areas whereby shoreline recession may modify and potentially accelerate pollutant inputs to coastal waters. This includes landfills (both historic and currently operating) (Brand et al., 2018; Stefania et al., 2019) as well as industrial sites including Superfund sites which are the most contaminated sites in the United States (Carter, 2020).

4 Conclusions

This study showed the impact of shoreline recession in modifying the fate of groundwater pollutants discharging to coastal waters at a specific study site, and discussed the broader potential implications for inland and marine coastal waters. The study findings show that the shoreline recession may accelerate the discharge of groundwater pollutants to coastal waters by decreasing the subsurface travel distance and travel time. In addition, shoreline recession may modify reactive processes close to the sediment-water interface, which may in turn affect the fate of reactive pollutants and their discharge to coastal waters. Importantly, shoreline recession may result in a landward shift of the recirculation zone that commonly exists close to the shoreline, and in doing so, alter the stability and abundance of sediment phases (e.g., Fe oxides) that often act to sequester pollutants and potentially limit their release to coastal waters. In particular, the study findings show that amorphous Fe oxides may be particularly impacted by the shoreline recession and may

take time to reform and function to sequester pollutants along the modified groundwater discharge pathway.

As it is expected that climate change will accelerate shoreline recession on coastlines worldwide due to increase in the magnitude of lake water level fluctuations, sea level rise, as well as increased frequency and intensity of storm events, it is recommended that future work evaluate the impact of shoreline changes of different time scales (e.g., event based, yearly, decadal) on pollutant fate in nearshore aquifers. The nearshore aquifer at the study site was relatively homogeneous and predominantly oxidizing and it is recommended that future studies evaluate the impact of shoreline recession in different nearshore aquifer types including more heterogeneous aquifers and those with more reducing conditions. Further, while this study focused on a freshwater coastal aquifer, field investigations are required to determine the impact of shoreline recession on the functioning of the reaction zone in nearshore aquifers along marine shorelines (i.e., subterranean estuary) and the corresponding impact on pollutant fluxes to marine waters. As the study data also demonstrate that the abundance and form of solid phase Fe near the shoreline may vary in response to shoreline change, there is a need to better understand the mineralization process for Fe oxides to better predict the impact of future changes on their functioning especially with respect to sequestering and releasing pollutants of concern. While this study focused on the impact of shoreline recession on nutrients derived from a septic system, it is recommended that future studies explore the potential impacts of shoreline recession on the discharge of other anthropogenic pollutants of concern that are commonly elevated in coastal groundwater systems.

Acknowledgements

This research was supported by a Natural Sciences and Engineering Research Council of Canada (NSERC) CREATE Grant (449311-2014), NSERC Strategic Grant (STPGP 430698-12) and NSERC Discovery Grant (03686-2015).

References

Adams, K.D., Minor, T.B., 2002. Historic shoreline change at Lake Tahoe from 1938 to 1998 and its impact on sediment and nutrient loading. J. Coast. Res. 18, 637–651.

Akinbola, G.E., Adigun, M.O., Aduroja, O., 2013. Dithionite and oxalate extraction of iron and manganese in some basement complex soils of southwestern Nigeria. J. Exp. Sci. 4, 22–26

Anderson, T.R., Fletcher, C.H., Barbee, M.M., Frazer, L.N., Romine, B.M., 2015. Doubling of coastal erosion under rising sea level by mid-century in Hawaii. Nat. Hazards 78, 75–103. https://doi.org/10.1007/s11069-015-1698-6

Anwar, N., Robinson, C., Barry, D.A., 2014. Influence of tides and waves on the fate of nutrients in a nearshore aquifer: Numerical simulations. Adv. Water Resour. 73, 203–213. https://doi.org/10.1016/j.advwatres.2014.08.015

Argyilan, E.P., Forman, S.L., 2003. Lake level response to seasonal climatic variability in the Lake Michigan-Huron system from 1920 to 1995. J. Great Lakes Res. 29, 488–500. https://doi.org/10.1016/S0380-1330(03)70453-5

Beck, A.J., Kellum, A.A., Luek, J.L., Cochran, M.A., 2016. Chemical flux associated with spatially and temporally variable submarine groundwater discharge, and chemical modification in the subterranean estuary at Gloucester Point, VA (USA). Estuaries and Coasts 39, 1–12. https://doi.org/10.1007/s12237-015-9972-0

Beck, M., Dellwig, O., Schnetger, B., Brumsack, H.J., 2008. Cycling of trace metals (Mn, Fe, Mo, U, V, Cr) in deep pore waters of intertidal flat sediments. Geochim. Cosmochim. Acta 72, 2822–2840. https://doi.org/10.1016/j.gca.2008.04.013

Bełdowska, M., Bełdowski, J., Kwasigroch, U., Szubska, M., Jędruch, A., 2022. Coastal cliff erosion as a source of toxic, essential and nonessential metals in the marine environment. Oceanologia. https://doi.org/10.1016/j.oceano.2022.04.001

Bird, E.C.., 2008. Coastal geomorphology, Second Edition. John Wiley & Sons Ltd. West Sussexx. England.

Brand, J.H., Spencer, K.L., O'shea, F.T., Lindsay, J.E., 2018. Potential pollution risks of historic landfills on low-lying coasts and estuaries. WIREs Water 5, 1–12. https://doi.org/10.1002/wat2.1264

Braun, K.N., Theuerkauf, E.J., Masterson, A.L., Curry, B.B., Horton, D.E., 2019. Modeling organic carbon loss from a rapidly eroding freshwater coastal wetland. Sci. Rep. 9, 1–13. https://doi.org/10.1038/s41598-019-40855-5

Brooks, S.M., Spencer, T., Christie, E.K., 2017. Storm impacts and shoreline recovery: Mechanisms and controls in the southern North Sea. Geomorphology 283, 48–60. https://doi.org/10.1016/j.geomorph.2017.01.007

Bruun, P., 1962. Sea-level rise as a cause of shore erosion. J. Waterw. Harb. Div. 88. https://doi.org/10.1061/JWHEAU.0000252

Burningham, H., French, J., 2017. Understanding coastal change using shoreline trend analysis supported by cluster-based segmentation. Geomorphology 282, 131–149. https://doi.org/10.1016/j.geomorph.2016.12.029

Canadian Council of Ministers of the Environment, 2014. Canadian Water Quality Guidelines for the Protection of Aquatic Life.

Carter, Jacob, Casey Kalman. 2020. A toxic relationship: Extreme coastal flooding and Superfund sites. Cambridge, MA: Union of Concerned Scientists. https://www.ucsusa.org/resources/toxic-relationship

Castedo, R., Fernández, M., Trenhaile, A.S., Paredes, C., 2013. Modeling cyclic recession of cohesive clay coasts: Effects of wave erosion and bluff stability. Mar. Geol. 335, 162–176. https://doi.org/10.1016/j.margeo.2012.11.001

Charette, M.A., Sholkovitz, E.R., 2002. Oxidative precipitation of groundwater-derived ferrous iron in the subterranean estuary of a coastal bay. Geophys. Res. Lett. 29, 85-1-85–4. https://doi.org/10.1029/2001gl014512

Davidson, M.A., Turner, I.L., Splinter, K.D., Harley, M.D., 2017. Annual prediction of shoreline erosion and subsequent recovery. Coast. Eng. 130, 14–25. https://doi.org/10.1016/j.coastaleng.2017.09.008

Dean, R.G., Houston, J.R., 2016. Determining shoreline response to sea level rise. Coast. Eng. 114, 1–8. https://doi.org/10.1016/j.coastaleng.2016.03.009

Dean, W.E., Neff, B.P., Rosenberry, D.O., Winter, T.C., Parkhurst, R., 2003. The significance of groundwater to the accumulation of iron and manganese in the sediments of two hydrologically distinct lakes in North-Central Minnesota: a geological perspective. GroundWater 41, 951–963. https://doi.org/10.1111/j.1745-6584.2003.tb02437.x

Department of Environment, Great Lakes and Energy, 2022. Septic Smart

https://www.michigan.gov/egle/about/organization/drinking-water-and-environmental-health/onsite-wastewater-management/septicsmart

Department of Fisheries and Oceans Canada Buoy, 2014. C45149 Southern Lake Huron http://www.meds-sdmm.dfo-mpo.gc.ca/isdm-gdsi/waves-vagues/data-donnees/index-eng.asp

DeRabbie, D., 2020. Septic Systems and Homeowner Insurance. Ontario Onsite Wastewater Association Newsletter, 15, 1. https://www.oowa.org/wp-content/uploads/2020/05/R_Vol15_Iss1.pdf

Destouni, G., Persson, K., Prieto, C., Jarsjö, J., 2010. General quantification of catchment-scale nutrient and pollutant transport through the subsurface to surface and coastal waters. Environ. Sci. Technol. 44, 2048–2055. https://doi.org/10.1021/es902338y

Eyles, N., Meulendyk, T., 2012. Ground-penetrating radar stratigraphy and depositional model for evolving Late Holocene aeolian dunes on the Lake Huron coast, Ontario. J. Great Lakes Res. 38, 708–719. https://doi.org/10.1016/j.jglr.2012.09.003

Fuller, C.C., Dadis, J.A., Waychunas, G.A., 1993. Surface chemistry of ferrihydrite: Part 2. Kinetics of arsenate adsorption and coprecipitation. Geochim. Cosmochim. Acta 57, 2271–2282. https://doi.org/10.1016/0016-7037(93)90568-H

García-Rubio, G., Huntley, D., Russell, P., 2015. Evaluating shoreline identification using optical satellite images. Mar. Geol. 359, 96–105. https://doi.org/10.1016/j.margeo.2014.11.002

Government of Canada - Environment and Climate Change Canada, U.S. EPA, 2009. Nearshore areas of the Great Lakes. https://doi.org/978-1-100-13563-2

Gronewold, A.D., Do, H.X., Mei, Y., Stow, C.A., 2021. A tug-of-war within the hydrologic

cycle of a continental freshwater basin. Geophys. Res. Lett. 48, 1–8. https://doi.org/10.1029/2020GL090374

Gronewold, A.D., Rood, R.B., 2019. Recent water level changes across Earth's largest lake system and implications for future variability. J. Great Lakes Res. 45, 1–3. https://doi.org/10.1016/j.jglr.2018.10.012

Gronewold, A.D., Stow, C.A., 2014. Water loss from the Great Lakes. Science (80-.). 343, 1084–1085. https://doi.org/10.1126/science.1249978

Hagenaars, G., de Vries, S., Luijendijk, A.P., de Boer, W.P., Reniers, A.J.H.M., 2018. On the accuracy of automated shoreline detection derived from satellite imagery: A case study of the sand motor mega-scale nourishment. Coast. Eng. 133, 113–125. https://doi.org/10.1016/j.coastaleng.2017.12.011

Hewlett, C., North, R.L., Johansson, J., Vandergucht, D.M., Hudson, J.J., 2015. Contribution of shoreline erosion to nutrient loading of the Lake Diefenbaker reservoir, Saskatchewan, Canada. J. Great Lakes Res. 41, 110–117. https://doi.org/10.1016/j.jglr.2014.11.020

Howard, K.W.F., Livingstone, S., 2000. Transport of urban contaminants into Lake Ontario via sub-surface flow. Urban Water 2, 183–195.

https://doi.org/10.1016/S1462-0758(00)00058-3

Kaczmarek, H., Mazaeva, O.A., Kozyreva, E.A., Babicheva, V.A., Tyszkowski, S., Rybchenko, A.A., Brykała, D., Bartczak, A., Słowiński, M., 2016. Impact of large water level fluctuations on geomorphological processes and their interactions in the shore zone of a dam reservoir. J. Great Lakes Res. 42, 926–941. https://doi.org/10.1016/j.jglr.2016.07.024

Kayastha, M.B., Ye, X., Huang, C., Xue, P., 2022. Future rise of the Great Lakes water levels under climate change. J. Hydrol. 612, 128205. https://doi.org/10.1016/j.jhydrol.2022.128205

Kopp, R.E., Horton, R.M., Little, C.M., Mitrovica, J.X., Oppenheimer, M., Rasmussen, D.J., Strauss, B.H., Tebaldi, C., 2014. Probabilistic 21st and 22nd century sea-level projections at a global network of tide-gauge sites. Earth's Futur. 2, 383–406. https://doi.org/10.1002/2014ef000239

Krueger, R., Zoet, L.K., Rawling, J.E., 2020. Coastal Bluff Evolution in Response to a Rapid Rise in Surface Water Level. J. Geophys. Res. Earth Surf. 125, 1–16. https://doi.org/10.1029/2019JF005428

Lee, J., Robinson, C., Couture, R.M., 2014. Effect of groundwater-lake interactions on arsenic enrichment in freshwater beach aquifers. Environ. Sci. Technol. 48, 10174–10181. https://doi.org/10.1021/es5020136

Lewandowski, J., Meinikmann, K., Nuetzmann, G., Rosenberry, D.O., 2015. Groundwater - the disregarded component in lake water and nutrient budgets. Part 2: Effects of groundwater on nutrients. Hydrol. Process. 29, 2922–2955. https://doi.org/10.1002/hyp.10384

Linkhorst, A., Dittmar, T., Waska, H., 2017. Molecular Fractionation of Dissolved Organic Matter in a Shallow Subterranean Estuary: The Role of the Iron Curtain. Environ. Sci. Technol. 51, 1312–1320. https://doi.org/10.1021/acs.est.6b03608

Luijendijk, A., Hagenaars, G., Ranasinghe, R., Baart, F., Donchyts, G., Aarninkhof, S., 2018. The State of the World's Beaches. Sci. Rep. 8, 1–11. https://doi.org/10.1038/s41598-018-24630-6

Malott, S., O'Carroll, D.M., Robinson, C.E., 2016. Dynamic groundwater flows and geochemistry in a sandy nearshore aquifer over a wave event. Water Resour. Res. 52, 5248–5264. https://doi.org/10.1002/2014WR015716

McAllister, S.M., Barnett, J.M., Heiss, J.W., Findlay, A.J., MacDonald, D.J., Dow, C.L., Luther, G.W., Michael, H.A., Chan, C.S., 2015. Dynamic hydrologic and biogeochemical processes drive microbially enhanced iron and sulfur cycling within the intertidal mixing zone of a beach aquifer. Limnol. Oceanogr. 60, 329–345. https://doi.org/10.1111/lno.10029

McKeague, J.A., Day, J.H., 1966. Dithionite and oxalate extractable Fe and Al as aids in differentiating various classes of soild. Can. J. Soil Sci. 46, 13–22. https://doi.org/10.4141/cjss66-003

Mehra, O.P., 1958. Iron oxide removal from soils and clays by a dithionite-citrate system buffered with sodium bicarbonate. Clays Clay Miner. 7, 317–327. https://doi.org/10.1346/ccmn.1958.0070122

Meile, C., Porubsky, W.P., Walker, R.L., Payne, K., 2010. Natural attenuation of nitrogen loading from septic effluents: Spatial and environmental controls. Water Res. 44, 1399–1408. https://doi.org/10.1016/j.watres.2009.11.019

Mitchell, M., Isdell, R.E., Herman, J., Tombleson, C., 2021. Impact Assessment and Management Challenges of Key Rural Human Health Infrastructure Under Sea Level Rise. Front. Mar. Sci. 8, 1–8. https://doi.org/10.3389/fmars.2021.631757

Moore, W.S., 2010. The effect of submarine groundwater discharge on the ocean. Ann. Rev. Mar. Sci. 2, 59–88. https://doi.org/10.1146/annurev-marine-120308-081019

Mukhopadhyay, A., Ghosh, P., Chanda, A., Ghosh, A., Ghosh, S., Das, S., Ghosh, T., Hazra, S., 2018. Threats to coastal communities of Mahanadi delta due to imminent consequences of erosion – Present and near future. Sci. Total Environ. 637–638, 717–729. https://doi.org/10.1016/j.scitotenv.2018.05.076

Nielsen, P., 2009. Coastal and Estuarine Processes. World Scientific, Singapore. https://doi.org/10.1142/7114

Nisbeth, C.S., Jessen, S., Bennike, O., Kidmose, J., Reitzel, K., 2019. Role of groundwater-borne geogenic phosphorus for the internal P release in shallow lakes. Water (Switzerland) 11, 1–16. https://doi.org/10.3390/w11091783

Niswonger, R.G., Panday, S., Motomu, I., 2011. MODFLOW-NWT , A Newton formulation for MODFLOW-2005. USGS reports 44.

Rakhimbekova, S., O'Carroll, D.M., Andersen, M.S., Wu, M.Z., Robinson, C.E., 2018. Effect of transient wave forcing on the behavior of arsenic in a nearshore aquifer. Environ. Sci. Technol. 52, 12338–12348. https://doi.org/10.1021/acs.est.8b03659

Rakhimbekova, S., O'Carroll, D.M., Oldfield, L.E., Ptacek, C.J., Robinson, C.E., 2021a. Spatiotemporal controls on septic system derived nutrients in a nearshore aquifer and their discharge to a large lake. Sci. Total Environ. 752. https://doi.org/10.1016/j.scitotenv.2020.141262

Rakhimbekova, S., O'Carroll, D.M., Robinson, C.E., 2021b. Factors controlling phosphorus mobility in nearshore aquifers adjacent to large lakes. Sci. Total Environ. 799, 149443. https://doi.org/10.1016/j.scitotenv.2021.149443

Rakhimbekova, S., O'Carroll, D.M., Robinson, C.E., 2021c. Occurrence of arsenic in nearshore aquifers adjacent to large inland lakes. Environ. Sci. Technol. https://doi.org/10.1021/acs.est.1c02326

Robinson, C., 2015. Review on groundwater as a source of nutrients to the Great Lakes and their tributaries. J. Great Lakes Res. 41, 941–950. https://doi.org/10.1016/j.jglr.2015.08.001

Robinson, C.E., Xin, P., Santos, I.R., Charette, M.A., Li, L., Barry, D.A., 2018. Groundwater dynamics in subterranean estuaries of coastal unconfined aquifers: Controls on submarine groundwater discharge and chemical inputs to the ocean. Adv. Water Resour. 115, 315–331. https://doi.org/10.1016/j.advwatres.2017.10.041

Rosenberry, D.O., Lewandowski, J., Meinikmann, K., Nützmann, G., 2015. Groundwater - the disregarded component in lake water and nutrient budgets . Part 1 : effects of groundwater on hydrology. Hydrol. Process. 2921, 2895–2921. https://doi.org/10.1002/hyp.10403

Roy, J.W., 2019. Endobenthic organisms exposed to chronically high chloride from groundwater discharging along freshwater urban streams and lakeshores. Environ. Sci. Technol. 53, 9389–9397. https://doi.org/10.1021/acs.est.9b02288

Roy, J.W., Malenica, A., 2013. Nutrients and toxic contaminants in shallow groundwater along Lake Simcoe urban shorelines. Inl. Waters. https://doi.org/10.5268/IW-3.2.521

Schwertmann, U., 1964. Differenzierung der eisenoxide des bodens durch extraktion mit ammonium-losung. https://doi.org/10.1002/jpln.3591050303

Sellinger, C.E., Stow, C.A., Lamon, E.C., Qian, S.S., 2008. Recent water level declines in the Lake Michigan-Huron system. Environ. Sci. Technol. 42, 367–373.

https://doi.org/10.1021/es070664+

Sirois, M., Couturier, M., Barber, A., Gélinas, Y., Chaillou, G., 2018. Interactions between iron and organic carbon in a sandy beach subterranean estuary. Mar. Chem. 202, 86–96. https://doi.org/10.1016/j.marchem.2018.02.004

Small, C., Nicholls, R.J., 2003. A global analysis of human settlement in coastal zones. J. Coast. Res. 19, 584–599.

Spiteri, C., Regnier, P., Slomp, C.P., Charette, M.A., 2006. pH-Dependent iron oxide precipitation in a subterranean estuary. J. Geochemical Explor. 88, 399–403. https://doi.org/10.1016/j.gexplo.2005.08.084

Spiteri, C., Slomp, C.P., Charette, M.A., Tuncay, K., Meile, C., 2008. Flow and nutrient dynamics in a subterranean estuary (Waquoit Bay, MA, USA): Field data and reactive transport modeling. Geochim. Cosmochim. Acta 72, 3398–3412. https://doi.org/10.1016/j.gca.2008.04.027

Stefania, G.A., Rotiroti, M., Buerge, I.J., Zanotti, C., Nava, V., Leoni, B., Fumagalli, L., Bonomi, T., 2019. Identification of groundwater pollution sources in a landfill site using artificial sweeteners, multivariate analysis and transport modeling. Waste Manag. 95, 116–128. https://doi.org/10.1016/j.wasman.2019.06.010

Swenson, M.J., Wu, C.H., Edil, T.B., Mickelson, D.M., 2006. Bluff recession rates and wave impact along the Wisconsin coast of Lake Superior. J. Great Lakes Res. 32, 512–530. https://doi.org/10.3394/0380-1330(2006)32[512:BRRAWI]2.0.CO;2

Theuerkauf, E.J., Braun, K.N., Nelson, D.M., Kaplan, M., Vivirito, S., Williams, J.D., 2019.

Coastal geomorphic response to seasonal water-level rise in the Laurentian Great Lakes: An example from Illinois Beach State Park, USA. J. Great Lakes Res. 45, 1055–1068. https://doi.org/10.1016/j.jglr.2019.09.012

US EPA, 1996. Method 3050B Acid digestion of sediments, sludges and soils, Method 3050B Acid digestion of sediments, sludges and soils.

Vitousek, S., Barnar, P.L., Fletcher, C.H., Frazer, N., Storlazzi, C.D., 2017. Doubling of coastal flooding frequency within decades due to sea-level rise 1–9. https://doi.org/10.1038/s41598-017-01362-7

Vogel, L.J., O'Carroll, D.M., Edge, T.A., Robinson, C.E., 2016. Release of Escherichia coli from Foreshore Sand and Pore Water during Intensified Wave Conditions at a Recreational Beach. Environ. Sci. Technol. 50, 5676–5684. https://doi.org/10.1021/acs.est.6b00707

Vousdoukas, M.I., Ranasinghe, R., Mentaschi, L., Plomaritis, T.A., Athanasiou, P., Luijendijk, A., Feyen, L., 2020. Sandy coastlines under threat of erosion. Nat. Clim. Chang. 10, 260–263. https://doi.org/10.1038/s41558-020-0697-0

Yi, S., Sun, W., Heki, K., Qian, A., 2015. An increase in the rate of global mean sea level rise since 2010. Geophys. Res. Lett. 42, 3998–4006. https://doi.org/10.1002/2015GL063902

Potential for shoreline recession to accelerate discharge of groundwater pollutants to coastal waters

Sabina Rakhimbekova[a*], Christopher Power[a], Denis M. O'Carroll[b], Clare E. Robinson[a]

[a] Department of Civil and Environmental Engineering, Western University, London, ON, Canada.

email: srakhimb@uwo.ca

[b] School of Civil and Environmental Engineering, Water Research Laboratory, University of New South Wales, Manly Vale, NSW 2093, Australia.

*corresponding author: Dr. Sabina Rakhimbekova

Key points:

- Increase in inland coastal water level resulted in ~ 30 m shoreline recession
- Shoreline recession accelerated PO_4-P discharge due to reduced travel paths
- Geochemical conditions near the shoreline governed fate and discharge of NO_3-N
- Shoreline recession modified location of "iron curtain"

Abstract

Discharge of groundwater-derived pollutants to inland and marine coastal waters is influenced by the transport and reactive processes occurring in nearshore aquifers. The effect of shoreline change on these processes and subsequent discharge of pollutants to coastal waters is unclear. The objective of this study was to evaluate the impact of shoreline recession (landward movement of the mean shoreline) on the transport of nitrogen [N] and phosphorus [P] in a nearshore aquifer and their discharge to coastal waters. Field investigations were conducted on a permeable unconfined nearshore aquifer on Lake Huron, Canada, in years coinciding with historically low and high lake water levels. At the site, a septic system-derived nutrient-rich (N and P) groundwater plume is moving towards the lake and the mean shoreline position moved ~30 m landward between sampling years due coastal erosion and mean lake water level increase. Data indicate PO_4-P fluxes to the lake were higher following shoreline recession due to shortened travel pathways. In contrast, NO_3-N fluxes were governed by the specific geochemical conditions near the sediment-water interface, which are not only a function of the shoreline position. Further, findings show shoreline recession may modify mineral phases that tend to sequester pollutants (e.g., iron oxides) near the sediment-water interface and this may possibly mediate release of sediment-bound pollutants. The findings provide new insights into potential impacts of shoreline change on chemical discharge to coastal waters as needed to inform long-term water quality predictions and management.

Keywords: climate change, shoreline erosion, coastal water level change, nutrients, iron curtain, septic system

1 Introduction

Coastal zones are the most populated and developed areas worldwide. Currently over half of the global population resides in coastal areas and this is expected to increase in the future based on current trends of coastal migration and population growth (Small and Nicholls, 2003). Sandy beaches, which occur along marine coastlines and along inland coastlines that are adjacent to large inland lakes, make up more than one-third of the ice-free global coastline (Luijendijk et al., 2018). Many sandy coastlines worldwide are threatened by the landward movement of the shoreline, known as shoreline recession. Shoreline recession, which is caused by increases in coastal water levels (i.e. sea level rise or lake level changes) combined with shoreline erosion, is expected to increase as the climate changes (e.g., higher frequency and more intense storm events) and in response to anthropogenic development (Bird, 2008). Luijendijk et al. (2018) found from satellite image analysis that 24% of the world's sandy beaches are eroding at rates exceeding 0.5 m/yr, with only 48% of sandy beaches considered stable. For the Laurentian Great Lakes, which have more than 6000 km of permeable shoreline (Government of Canada - Environment and Climate Change Canada and U.S. EPA, 2009), shoreline recession caused by interannual lake water level fluctuations combined with erosive storm events is an increasing challenge. Lake water level fluctuations up to one to two meters occur along large lacustrine shorelines, such as the Great Lakes, approximately once a decade (Argyilan and Forman, 2003; Sellinger et al., 2008).

It is well established that shoreline recession along marine and inland coastlines has severe economic, social and environmental consequences due to impacts including land and habitat loss, property damage, and reduced revenue potential from tourism and industry

(Mukhopadhyay et al., 2018; Theuerkauf et al., 2019). As such, this is an active area of research, with studies generally focused on monitoring shoreline changes (e.g. Burningham and French, 2017; García-Rubio et al., 2015; Hagenaars et al., 2018), fundamental understanding of underlying geomorphological and hydrological processes (e.g. Brooks et al., 2017; Swenson et al., 2006), and techniques for forecasting shoreline change over short and long time scales (e.g. Davidson et al., 2017; Mukhopadhyay et al., 2018). Few studies have examined the potential impacts of shoreline recession, including sediment erosion and changes in coastal water levels, on the flux of land-derived pollutants to coastal waters. Two prior studies examined on the impact of shoreline erosion on nutrient loading to Lake Tahoe, United States (Adams and Minor, 2002) and Lake Diefenbaker Reservoir, Canada (Hewlett et al., 2015). Both studies found that nutrient loading caused by shoreline erosion (due to release of sediment-bound nutrients) only contributed a fraction of the total nutrient load into the lakes (< 5% of total nutrient input). More recently, beach sand erosion was found to be the main mechanism of transferring *E.coli* to nearshore coastal waters during intensified wave conditions at a sandy beaches (Vogel et al., 2016). Finally, focused on a coastal wetlands rather than sandy shorelines, Braun et al. (2019) showed that shoreline recession may reduce the carbon storage potential of a coastal wetland and thereby impact carbon dynamics within the wetland. The above-mentioned studies all focus on sediment-bound pollutants that are released to coastal waters as sediment near the shoreline is eroded and released to the coastal waters. While this can be an important transport mechanism, shoreline recession may also affect the delivery of dissolved pollutants into coastal waters, particularly land-derived groundwater pollutants, whose delivery to coastal waters strongly depends on the specific subsurface transport pathways between the land source and coastal

waters, as well as the geochemical conditions along these pathways in nearshore aquifers (Bełdowska et al., 2022; Destouni et al., 2010). For instance, shoreline recession brings the shoreline closer to areas of human development (e.g. infrastructure, landfills, and contaminated sites), which decreases the distance between a groundwater pollution source and the coastal water. This may in turn increase the potential for groundwater-derived pollutants reaching coastal waters.

Submarine groundwater discharge (SGD) and lacustrine groundwater discharge (LGD) are important pathways for land-derived pollutants such as nutrients, metals and organic contaminants to enter marine and inland coastal waters, respectively (e.g. Beck et al., 2016; Lewandowski et al., 2015; Moore, 2010). With increased urbanization, industrialization and intensification of agriculture in coastal areas, groundwater pollutant concentrations can be high in coastal areas and pose a risk to coastal water pollution. The importance of LGD has mainly been recognized for its contribution to lake nutrient loads and lake eutrophication (Robinson, 2015; Rosenberry et al., 2015). For instance, high nutrient concentrations, more than ten times higher than in the adjacent lake water, were observed in groundwater discharging into Lake Simcoe (Roy and Malenica, 2013). In addition to nutrients, studies have also shown that LGD may play an important role in delivering other chemical constituents, including metals (Lee et al., 2014; Rakhimbekova et al., 2018) and road salt (Howard and Livingstone, 2000; Roy, 2019) to lakes. The transport of pollutants via groundwater flow paths to coastal waters is generally slow, and transport can be retarded by various physical and chemical processes (e.g. filtration, sorption, precipitation). Therefore, changes in the shoreline position may impact the groundwater travel times, travel distances and the specific pathways, by which pollutant are transported

from their land source to coastal waters. In addition, it is well established that an important reaction zone can exist in nearshore aquifers close to the shoreline due to the mixing of groundwater and coastal water. This zone, commonly referred to as a subterranean estuary in marine environments, is known to strongly influence the discharge of groundwater-derived pollutants to coastal waters due to its high reactivity (Rakhimbekova et al., 2021b, 2021c; Robinson et al., 2018). One important reactive phenomenon in this mixing zone is the sequestration (trapping) of pollutants to sediment mineral phases, particularly iron (Fe) oxides, which form under certain redox and pH conditions. This sediment trap mechanism, commonly referred to as the "iron curtain", can act as a natural barrier that limits the release of a range of pollutants, including phosphorus (Charette and Sholkovitz, 2002; Spiteri et al., 2008), carbon (Linkhorst et al., 2017; Sirois et al., 2018), metals (McAllister et al., 2015), and trace metals (Beck et al., 2008) to coastal waters. It is possible shoreline recession may cause a shift in the location of the mixing zone, thereby impacting reactivity and geochemical conditions, including the function of sediment trap and its ability to sequester pollutants. This may in turn modify pollutant fluxes delivered to coastal waters via SGD and LGD.

To the best of our knowledge, there are no studies that have explored the impact of shoreline changes, including shoreline recession, on the discharge of groundwater-derived pollutants to coastal waters. The objective of this study is to address this knowledge gap. Field data collected downgradient of a large septic system over a six-year period is used to examine the influence of shoreline recession on the subsurface transport of a P- and N-rich wastewater plume and its potential discharge to the adjacent lake. In addition, the study investigates the way in which shoreline recession may alter geochemical conditions near

the sediment-water interface with a specific focus on the abundance and distribution of mineral phases that tend to sequester pollutants, including P, close to the groundwater-coastal water interface. Finally, this study explores the broader possible impacts of shoreline recession beyond our specific study site by discussion of potential sources of anthropogenic groundwater contaminant sources along shorelines and future projections on lake water level changes and expected shoreline changes. The findings of this study are needed given the prevalence of groundwater contamination near marine and inland coastlines, and the projected changes in coastal water levels and storm intensity and frequency as the climate changes.

2 Methodology

2.1 Field investigation

2.1.1 Site description

Field investigations were conducted at Ipperwash Beach on Lake Huron, Ontario, Canada in 2014, 2015, and 2020 (Figure 1a). Ipperwash Beach is a sandy beach that extends over 20 km and has an extensive dune system behind the beach that rises several meters above the lake surface (Eyles and Meulendyk, 2012). Extensive shoreline recession occurred at Ipperwash Beach between 2015 and 2020 in response to an increase in the water level in Lake Huron combined with beach erosion. In 2020, the water level in Lake Huron reached 177.45 m (IGLD 85 datum) following over a decade of low water levels during which the record low water level of 175.57 m occurred in 2013 (Gronewold et al., 2021; Gronewold and Stow, 2014). The extent of shoreline recession between 2015 and 2020 are illustrated in aerial photographs shown in Figure 1b.

Ipperwash Beach was selected for this study as a public comfort station with a large septic system is located in close vicinity to the beach (Figure 1b). The septic system has been operational since at least 1974 and is only used during the warmer months from May to September. Due to shoreline recession, the mean shoreline position was located ~120 m from the septic system tile bed in 2015, but only ~90 m from the septic tile bed in 2020 (Figure 1b). Detailed (approximately monthly) field sampling was conducted between August and October in 2014, and between May and August in 2015, to evaluate the spatial and temporal variability of phosphorus (P) and nitrogen (N) transport from the septic system through the nearshore aquifer to the lake. Details of this previous study are provided in Rakhimbekova et al. (2021a). This current study expands upon this prior work with new sampling performed in 2020 to determine the impact of shoreline recession on the transport of P and N through the nearshore aquifer and their potential discharge to the lake.

2.1.2 *Field monitoring approach*

2.1.2.1 *Field equipment*

For all sampling periods in 2014-2015 and 2020, a cross-shore monitoring transect was installed that aligned with the center of the septic system-derived nutrient-rich plume that is moving towards the lake. The original cross-shore monitoring transect in 2014-2015 consisted of ten multi-level samplers (MLS) and extended from ~71 m downgradient of the septic tile bed (x = 71 m; landward extent of the beach dunes) to ~20 m offshore (x = 140 m; Figure 1c). For the 2020 sampling, the cross-shore monitoring transect consisted of six MLS, and extended from x = 71 m downgradient of septic tile bed ~20 m offshore (x = 110 m) (Figure 1c). The x-z coordinate system used herein is defined with x = 0 m located at the landward edge of the septic tile bed and z = 0 as the elevation of a local permanent

benchmark. All MLS were installed up to 3 m below ground surface, with sampling ports at 0.2 m depth intervals.

Two piezometers (PZ) were permanently installed at x = 71 m (PZ-1) and x = 93 m (PZ-2) in July 2014, with additional piezometers temporarily installed along the cross-shore monitoring transect at the start of each sampling event to measure the groundwater and lake water levels across the nearshore aquifer and offshore. The location of monitoring equipment and ground surface elevations were surveyed with a total station (Topcon GTS-239W) relative to a local permanent benchmark during each sampling event (Figure 1c).

2.1.2.2 *Electrical resistivity imaging*

The septic system origin of the nutrient-rich plume observed in the nearshore aquifer was confirmed in 2015 by using artificial sweeteners as a chemical tracer for human wastewater (Rakhimbekova et al., 2021a). However, the artificial sweetener data were limited to point information obtained from samples collected at selected MLS located over 70 m downgradient of the septic tile bed (i.e., samples collected from x = 71 m onwards). During the field sampling in 2020, a non-invasive electrical resistivity tomography (ERT) survey was performed to provide continuous imaging of electrical resistivity within the subsurface and determine if this approach would be able to trace the nutrient-rich plume back to the septic tile beds.

An ERT survey line consisting of 96 stainless-steel electrodes (0.3 m) with an inline spacing of 1 m was deployed. The location of the line coincided with the location of the cross-shore monitoring transect but it extended from the landward edge of the septic tile bed (x = 0 m) to the shoreline (x = 95 m) (Figure 1b). A multi-channel Syscal Pro Switch

48 resistivity system (IRIS Instruments, France) was used to complete the survey. As this system is limited to 48 electrodes at a time, the roll-along method was used to record the survey line through three successive segments. For this, 24 electrodes were moved for each segment to ensure 50% overlap (i.e., electrode numbers: 0-48, 24-72, 48-96) (Robinson et al., 2022).

The multi-gradient electrode array was used with a total of 4183 measurements. Due to the dry surface sand, saline water was added around each electrode to ensure strong ground coupling (resistance: <1 kilo-ohm). The recorded apparent resistivity data was inverted with DC_2DPro, an iterative least-squares smoothness-constrained inversion program (Kim, 2016). The surface elevation at each electrode, which was surveyed using the total station, was incorporated into the inversion, which was then run to a maximum of seven iterations, showing good convergence with a low root mean square (RMS) error of 5.5%.

2.1.2.3 *Porewater sampling and analysis*

For all sampling events, pore water samples were first collected from all MLS ports using syringes attached to the PVC sampling tubes (ϕ = 1.35 mm). Porewater samples were collected from each port, filtered using 0.45 µm cellulose acetate filters, and stored in 60 mL HDPE bottles. Samples were analyzed for phosphate (PO_4-P), nitrate (NO_3-N) and chloride (Cl) within 48 hours of collection. After samples were collected, a peristaltic pump was used to draw pore water directly into a flow cell where pH, electrical conductivity (EC) and temperature were measured with an In-Situ Multi-Parameter TROLL® 9500 and YSI 6600 V2 Sonde. Multiple nearshore lake water samples were also collected during each sampling event. Collected pore water samples were analyzed for nutrients (PO_4-P, NO_3-N)

using Lachat 750 Flow Injection Analysis (Lachat 750), and Cl using High Performance Liquid Chromatography.

2.1.2.4 *Sediment sampling and analysis*

During MLS installation in May 2015 and August 2020, multiple sediment samples were collected at depths of 0.5 m to 2 m below the ground surface for sediment chemistry characterization (Figure 1c). Sediment samples were analyzed via total acid digestion using method EPA 200.8 (US EPA, 1996) to determine the total elemental solid phase concentrations. In addition, due to the potential importance of Fe-bearing solid phases in sequestering chemical including P in nearshore aquifers, select sediment samples were treated with (i) acid ammonium oxalate solution (McKeague and Day, 1966), and (ii) dithionite-citrate-bicarbonate solution (Mehra, 1958) to provide characterization of the Fe-bearing solid phases (e.g. degree of crystallization). Oxalate-extractable Fe (Fe_o) is operationally thought to represent amorphous oxides such as ferrihydrite and small amounts of organically-bound Fe (Schwertmann, 1964). Dithionite-extractable Fe (Fe_d) is operationally thought to represent organically-bound oxides, amorphous oxides, and finely crystalline oxides (Akinbola et al., 2013). The difference between Fe_d and Fe_o generally represents the amount of solid phase Fe present in crystalline oxide forms (e.g., goethite and hematite). Total dissolved phosphorus (TDP) and total iron (Fe) in extractant solutions were analyzed using HACH DR 6000 UV VIS Spectrophotometer and inductively-coupled plasma mass spectroscopy (ICP-MS), respectively. Additional details on sediment sample analysis are provided in the Supporting Information (SI Section 1).

2.2 Numerical model

A two-dimensional (2D) model was developed in MODFLOW-NWT (Niswonger et al., 2011) to simulate steady state groundwater flows and estimate NO_3-N and PO_4-P loads discharging to the lake along the vertical cross-shore section. The model domain and parameterization were based on a groundwater model of the study site developed and validated by Malott et al. (2016). The two-dimensional model assumes negligible groundwater flow in the alongshore direction. The model was 150 m long in the cross-shore direction and the aquifer thickness at the shoreline location was set to 13 m at the landward boundary due to presence of a clay layer at this depth according to local well records (Figure 2). The beach face and lake boundaries (AB and BC) were specified based on topographic sand level surveys conducted during each sampling period. The model was discretized into 71 layers and 128 columns with greater refinement around the shoreline and the beach face. Grid discretization tests were performed to ensure a converged solution. Particle size analysis performed on sediment samples (n = 7) collected across the nearshore aquifer up to 2.5 m below the water table indicated that the nearshore aquifer is comprised of relatively homogeneous fine sand (Coefficient of Uniformity, C_u = 2.18 and sand grain size, d_{50} = 0.16 mm) with the saturated K estimated to range from 7 to 15 m/d using the method of Krumbein and Monk (1943). Based on this, the simulated aquifer was homogeneous and isotropic with the hydraulic conductivity (K) set to 10 m/d and effective porosity n = 0.3.

The upper (AB) and bottom (ED) model boundaries were no-flow boundaries assuming negligible aerial recharge and evaporation, and an impermeable aquifer basement, respectively. The offshore boundary (CD) was specified as no-flow boundary and was

located sufficiently far from the shoreline (>50 m offshore) that it did not influence the groundwater flows in the nearshore aquifer (Figure 2). The vertical landward boundary (AE) was located at x = 60 m, which is 10 m inland from the landward extent of the beach dunes (Figure 2) and was set to be a constant head boundary. Three simulations were run with the boundary conditions modified to represent the mean hydrological conditions at the study site during the 2014, 2015 and 2020 sampling periods. Based on the measured groundwater levels, the hydraulic head at the landward boundary was set to -2.95 m, -3.05 m and -1.95 m, respectively, for the models simulating the groundwater flows over the sampling periods in 2014, 2015 and 2020. A constant head condition was used along the lake boundary (BC) with the specified head values set based on the mean measured lake water level during each of the sampling periods and considering the effect of steady waves acting on the boundary. To simulate the effect of steady waves, the approach of Anwar et al. (2014) was adopted whereby the time-averaged effect of waves as described by wave set-up was used (details are provided in SI Section 2). For this, the empirical equation of Nielsen (2009) was used to estimate the wave-set up profile and calculate head values that were then prescribed along the lake boundary (BC). Offshore root mean square wave heights (H_{rms}) of 0.35 m, 0.25 m and 0.35 m were used in the equation of Nielsen (2009) to simulate the mean wave conditions over the sampling periods in 2014, 2015 and 2020, respectively. The mean H_{rms} values were calculated using monitoring data from a wave buoy located ~35 km from the study site (C45149 Southern Lake Huron, Department of Fisheries and Oceans Canada Buoy, 2020). Based on the mean lake water levels measured at the study site during the sampling periods in 2014, 2015 and 2020, the still lake water level in the models were set to -3.64 m, -3.73 m and -2.21 m, respectively.

3 Results and discussion

3.1 Field and modeling results

3.1.1 Change in hydrological conditions between sampling periods

The hydrological conditions at the study site including the mean lake water level, mean wave conditions, and landward groundwater levels varied between the sampling periods. The mean lake water level was approximately 0.7 m higher in 2020 compared to 2014-2015 (Figure 3a). More intensified wave conditions were also observed in 2020 compared to 2014-2015 with maximum wave height (H_{rms}) reaching 3.7 m in 2020 compared to 3.0 m in 2014 and 2.1 m in 2015 (mean H_{rms} was 0.35 m, 0.25 m and 0.35 m in 2020, 2015 and 2014, respectively; Figure 3b). The extent of shoreline recession between 2015 and 2020 is evident by comparing the topographical surveys performed in 2015 and 2020, along with corresponding aerial photographs (Figures 1b and 1c). The shoreline was estimated to move 30 m landward from x = 120-125 m in 2014-2015, to x = 90 m in 2020, in response to the lake water level increase and beach sand erosion.

Increase in lake water levels may lead to a corresponding increase in the landward groundwater table elevation, and thereby reduce the vertical separation between septic tile beds and groundwater table. This can be a concern as it then limits the efficiency of the septic tile bed in attenuating wastewater constituents including nutrients (Mitchell et al., 2021). Based on groundwater levels measured at PZ-1 (x = 71 m), there was ~ 1 m increase in the groundwater table between 2014-2015 and 2020 (Figure 1c). However, with high sand dunes behind the beach, there is a thick (3 - 4 m) vadose zone below the septic tile beds at this study site (see Section 3.1.2 for details), and therefore it is not expected that the higher groundwater table elevation in 2020 compared to 2014 – 2015 would have

adversely impacted the function of the vadose zone below the septic tile beds in attenuating wastewater constituents. The adverse impact of increasing coastal levels on the attenuation of wastewater constituents below the septic tile beds is expected to be a larger concern in coastal plain settings with flatter topography and shallow groundwater tables.

The mean hydraulic gradient across nearshore aquifer was negative in 2014-2015 (h = -0.015) and 2020 (h = -0.017), indicating lakeward groundwater flow. Based on the hydraulic gradient in 2014-2015 and 2020, mean hydraulic conductivity (K = 10 m/d) and effective porosity (n = 0.3) for the nearshore aquifer, the mean horizontal groundwater velocity towards the lake is estimated to be 0.50 m/d in 2014-2015 and 0.56 m/d in 2020. Numerical simulations show the change in groundwater flow patterns (Figure 4a-c) in the nearshore aquifer between the 2014-2015 and 2020 sampling periods with the groundwater discharge zone shifting from x = 120-125 m in 2014-2015 to x = 85-90 m in 2020. Based on the estimated overall mean horizontal velocities and shoreline positions, the travel time for conservative species to be transported from the septic tile bed to the shoreline is estimated to be around 240 days in 2014-2015 compared to only 160 days in 2020.

While the flow patterns simulated by the steady state groundwater models do not indicate recirculation of lake water through the nearshore aquifer (Figure 4a-c), recirculating flows driven mostly by changing lake water levels and wave conditions are expected to occur landward of the mean shoreline position and simulated groundwater discharge zone (Malott et al., 2016). With the mean shoreline position and zone of groundwater discharge shifting landward in 2020 compared to 2014-2015, the recirculation zone, which is generally associated with high reactivity including the presence of mineral phases (e.g., Fe oxides) that tend sequester pollutants (Lee et al., 2014; Lewandowski et al., 2015; Rakhimbekova

et al., 2018), would also have shifted landward. It is possible that this landward shift in the recirculation zone could have altered geochemical conditions in the nearshore aquifer and this is explored in the following sections.

3.1.2 Characterization of septic-derived nutrient plume

Elevated groundwater PO_4-P and NO_3–N concentrations were observed at the study site in 2014, 2015 and 2020 (Figures 4d to 4i). Groundwater PO_4-P concentrations ranged from 8 to 166 μg/L in 2014-2015, and from 3 to 98 μg/L in 2020. Maximum PO_4-P concentrations in the nearshore aquifer exceeded the upper limit of the Canadian Water Quality Guidelines for the Protection of Aquatic Life for Total Phosphorus to limit eutrophic conditions (35–100 μg P/L; Canadian Council of Ministers of the Environment, 2014), and were considerably higher than the mean measured lake water concentrations for all sampling periods (2-3 μg/L). Groundwater NO_3–N concentrations ranged from 4 to 57 mg/L in 2014-2015 and from 1 to 26 mg/L in 2020. Maximum NO_3-N concentrations in the nearshore aquifer exceeded the Canadian Water Quality Guidelines for the Protection of Aquatic Life for all sampling periods (3 mg/L; Canadian Council of Ministers of the Environment, 2014), and were also higher than the mean measured lake water concentrations (0.2-0.8 mg/L).

Figures 4j-l to 4m-o presents the distributions of chloride (Cl) concentrations and electrical conductivity (EC) measured along the monitoring transect in 2014, 2015 and 2020. Cl and EC can be considered conservative wastewater tracers at the site(Rakhimbekova et al., 2021a), and their distributions generally coincide with the locations of elevated PO_4-P and NO_3–N in the nearshore aquifer Figure 4d-i. NO_3–N with EC landward of the maximum shoreline position are correlated (Figure S1) indicating the suitability of using ERT for

characterizing the spatial extent of the high nutrient groundwater plume. Figure 5 shows a 2D cross-sectional ERT image that extends from x = 0 m (septic tile bed) to x = 95 m (near the mean shoreline position in 2020). The location of the septic tile bed, PZ-1 and MLS are indicated in the figure, along with the lake water and groundwater levels measured during the survey. The highly resistive near surface layer between x = 0 m and x = 78 m (red-purple; >1000 ohm-m) represents the vadose zone with a mean thickness of approximately 4 m. The underlying layer of low resistivity (blue-green; <150 ohm-m) represents the zone of saturated groundwater, with some areas having very low resistivity (<50 ohm-m). The ERT image can be validated by comparing bulk resistivity values with the porewater EC measurements in Figure 4m-o. For example, the porewater EC at x = 71 m and z = -3 m (PZ-1) is 1008 μS/cm which suggests a bulk EC of 209 μS/cm, or bulk resistivity of 48 ohm-m (Archie, 1942) – this closely matches the bulk resistivity inferred by ERT at that location (55 ohm-m). Figure 5 indicates that the zone of very low bulk resistivity is connected to the base of the septic tile bed and extends lakeward. This zone exists through the shallow nearshore aquifer and becomes shallower near the shoreline meeting the sediment-water interface around x = 92 m. This ERT image clearly illustrates that the elevated NO_3-N and PO_4-P concentrations observed near the shoreline originate from the septic tile bed.

3.1.3 Impact of shoreline recession on PO_4-P

As seen in Figure 4, the highest PO_4-P concentrations were observed 73-90 m lakeward of the septic tile bed (maximum PO_4-P = 166 μg/L; x = 73-90 m) in 2014-2015, with concentrations decreasing closer to the shoreline (particularly in 2015). However, elevated concentrations of the conservative wastewater tracers, Cl and EC, near the shoreline (x =

115-125 m) for these sampling periods suggest that the septic-derived wastewater plume has reached the shoreline. Taking into account septic system operation time, groundwater velocity, and length of the PO_4-P plume in 2015, Rakhimbekova et al. (2021) concluded that PO_4-P transport in the nearshore aquifer was mainly governed by retardation. Based on the location of the PO_4-P plume in 2015, it was predicted that PO_4-P may possibly reach the shoreline in approximately 10 years. However, this prediction is incorrect due to shoreline recession at the site. Figure 4f shows that in 2020 (within <5 years), the PO_4-P plume has reached the new shoreline location (x = 90 m). To provide a quantitative estimate on the extent to which PO_4-P fluxes to the lake may have changed, the measured PO_4-P concentrations were combined with the simulated groundwater flows for each sampling period. PO_4-P fluxes were calculated by multiplying PO_4-P concentrations (interpolated to a depth of 3 m below ground surface) along vertical line near the shoreline (x = 120.3 m in 2014 and 2015 and x = 88.7 m in 2020; Figure 4 a-c) by simulated groundwater fluxes directed towards the lake for each sampling year (Additional details provided in SM S3). From these calculations, it is estimated that the PO_4-P flux to the lake may have increased nearly tenfold from 53 mg/d/m in 2015 to 482 mg/d/m in 2020 (Figure 6a) due higher PO_4-P concentrations near the shoreline in 2020 compared to near the shoreline in 2015 as well as slightly higher lakeward-directed groundwater velocity (Figure 4e, f). This result illustrates that the shoreline recession can accelerate the discharge of groundwater-derived pollutants that are slowly advancing towards the shoreline by decreasing the subsurface travel distance and time.

3.1.4 Impact of shoreline recession on NO_3-N

The NO_3-N distribution in the nearshore aquifer was influenced by not only its shorter discharge pathway through the nearshore aquifer due to shoreline recession but also by the specific geochemical conditions near the sediment-water interface that impact reactive transformations that NO_3-N may undergo prior to its discharge. Rakhimbekova et al. (2021a) previously showed that the extent of NO_3-N removal that occurs in the nearshore aquifer prior to discharge may vary over time as the extent of denitrification changes in response to changing geochemical conditions near the sediment-water interface (e.g., due to changes in organic matter availability). Rakhimbekova et al. (2021a) presented detailed data analysis showing changing organic matter availability was associated with the observed decrease in NO_3–N concentrations near the shoreline in 2015 (0-2 mg/L) compared to 2014 (4-67 mg/L), and thus lower estimated NO_3-N flux towards the lake in 2015 (4 mg/d/m) compared to 2014 (124 mg/d/m) (Figure 6b).

NO_3–N concentrations observed near the mean shoreline position in 2020 (x = 85-90 m) ranged from 4 to 26 mg/L in 2020 (Figure 4i). The estimated NO_3-N flux directed towards the lake near the shoreline in 2020 (79 mg/d/m) was larger than in 2015 (4 mg/d/m) but smaller than in 2014 (124 mg/d/m). NO_3-N flux is affected by both groundwater velocity and NO_3-N concentrations. Since groundwater velocity near the shoreline was slightly higher in 2020 compared to 2014 (difference in flow arrow sizes in Figure 4 a-c), the higher estimated NO_3-N flux in 2014 is due to higher NO_3-N concentrations near the shoreline in 2014 compared to 2020. Therefore, even though shoreline recession reduced the travel distance and travel time for the septic-derived NO_3-N to reach the lake, the specific geochemical conditions in the nearshore aquifer near the shoreline ultimately govern the

flux of NO_3-N to the lake rather than the overall travel distance and time. This finding is in contrast to the highly retarded PO_4-P plume for which shoreline recession was found to directly accelerate PO_4-P discharge to the lake due to the overall reduced travel distance between the septic tile bed and shoreline.

It is important to note that while the geochemical conditions near the shoreline have a controlling influence on the fate of NO_3-N in the nearshore aquifer and its flux to the lake at our study site, this may not be the case at other sites. The nearshore aquifer at our study site (from the septic tile bed to shoreline) is predominantly oxic and therefore limited denitrification occurs as NO_3-N is transported towards the shoreline. At other sites where the nearshore aquifer is more reducing, it is possible that the decrease in overall travel distance and times could limit the extent of denitrification that occurs as NO_3-N is transported from the source to the coastal water (Meile et al., 2010). Further, it is possible that shoreline recession could have a greater impact on the discharge of reactive pollutants in nearshore aquifers with sharper geochemical (redox and pH) gradients than observed at Ipperwash Beach (Rakhimbekova et al., 2021a, 2018).

3.1.5 Impact of shoreline recession on Fe curtain processes

In addition to modifying the physical transport pathways and travel times for the septic-derived nutrients being transported towards to the lake, the change in shoreline location may also modify the geochemical conditions near the groundwater-lake interface. In particular, it may modify the distribution, abundance and reactivity of mineral phases that can sequester pollutants in the nearshore aquifer. Rakhimbekova et al. (2021b) showed elevated solid phase Fe and P exists in the nearshore aquifer at the study site and suggested that PO_4-P derived from the decomposition of lake-derived organic matter may be

accumulating on Fe oxide minerals that exist close to the sediment-water interface. Previous studies in marine environments have similarly found that Fe oxides that form near the sediment-water interface can act as a geochemical barrier (i.e. “iron curtain”) with these minerals sequestering pollutants such as PO_4-P and limiting their release to coastal waters(Charette and Sholkovitz, 2002; Spiteri et al., 2006). While it is thought that sequestered pollutants may later be re-mobilized if geochemical or hydrological conditions change (Nisbeth et al., 2019; Spiteri et al., 2006), in this section we examine how the distribution and abundance of solid phase P and Fe, including Fe oxides, in the nearshore aquifer may have changed in response to shoreline recession.

Rakhimbekova et al. (201b) previously showed that nearshore aquifer at the study site is predominantly oxidizing, and there is no distinct redox gradient near the sediment-water interface. Further, Fe oxides are available through the nearshore aquifer and tend to accumulate PO_4-P on their mineral surfaces. Characterization of the distribution of solid phase P and Fe in the nearshore aquifer at the study site in 2015 and 2020 indicate a decrease in solid phase P and Fe between these times (Figure 7a-d). Due to the landward movement of the shoreline, sediment samples were taken in different locations in 2015 compared with 2020. To enable comparison of P and Fe solid phase concentrations between two times, comparison only considers samples collected over the same area, between x = 87 and 117 m (marked with red square on Figure 7). Generally, there was higher abundance of solid phase P near the shoreline in 2015 compared to 2020 (151 ± 51 μg/g in 2015, n = 17; 82 ± 55 μg/g in 2020, n = 23; Figure 7a and b). Solid phase Fe was also slightly higher in 2015 compared to 2020 (3.1 ± 0.6 mg/g in 2015, n = 17; 2.7 ± 0.7 mg/g in 2020, n = 23; Figure 7c and d).

Selective solid phase extractions were conducted to characterize Fe-bearing solid phases (amorphous, Fe_o and more crystalline, Fe_d) at the study site in 2015 and 2020. Again, only sediment samples collected between x = 87 and 117 m were used to compare the distribution of amorphous and crystalline Fe phases in 2015 and 2020. The abundance of Fe_o decreased between 2015 and 2020 (0.5 ± 0.2 mg/g in 2015, n = 10; 0.2 ± 0.09 mg/g in 2020, n = 13; Figure 7e and f). In contrast, Fe_d was slightly higher in 2020 compared to 2015 (0.5 ± 0.07 mg/g in 2015; 0.7 mg/g ± 0.3 in 2020; Figure 7g vs 7h). Lower Fe_d in 2015 compared to 2020 may possibly be due to the formation of more crystalline Fe phases over time. Larger difference in the abundance of Fe_o compared to Fe_d between 2015 and 2020 suggest that shoreline recession may have larger impact on amorphous Fe oxides compared to crystalline Fe oxides. This is not unexpected given that amorphous Fe oxides are less stable and shoreline recession may have altered factors that affect Fe oxide stability (e.g. oxygen availability, presence of bacteria) (Charette and Sholkovitz, 2002; Dean et al., 2003). Following shoreline recession, particularly a large erosive event, it might take time for amorphous Fe oxides to reform around the new shoreline location. This may explain the lower Fe_o near the new shoreline location in 2020 compared to higher Fe_o near the location of shoreline in 2015, which was a more stable shoreline position over the preceding years.

Amorphous Fe (e.g. ferrihydrite) tend to have a higher surface area that is more reactive and therefore has a higher capacity to sequester pollutants, including PO_4-P, compared to more crystalline Fe oxides fractions such as goethite and hematite (Fuller et al., 1993). Therefore, lower abundance of Fe_o in the nearshore aquifer in 2020 (following the shoreline recession) suggests that mineral surfaces along the groundwater discharge pathway may

have less ability to sequester PO_4-P, and this may possibily lead to higher PO_4-P fluxes to lake. The impact of shoreline recession on the distribution and abundance of Fe oxide minerals, particularly amorphous Fe oxides, is important as it may affect the function of these minerals in sequestering and releasing pollutants thereby modifying pollutant fluxes to coastal waters.

3.2 Broader implications of the impact of shoreline recession

The study findings demonstrate the potential impacts of shoreline recession driven by coastal water level changes and/or erosion on the transport and fate of groundwater pollutants and their discharge to adjacent coastal waters. The findings show shoreline recession may impact pollutants moving slowly along groundwater pathways towards the coastal water, as well as pollutants for which their fate and ultimate delivery to coastal waters is governed strongly by the geochemical conditions in the reaction zone that exists near the groundwater-coastal water interface. This section explores the broader implications of the study findings on the discharge of groundwater pollutants to the Laurentian Great Lakes, as well as other inland and marine coastal waters.

While it is known that water levels in the Great Lakes vary over 20 – 30 year cycles (Gronewold and Rood, 2019), recent future projections estimate that by 2040-2049 average annual water levels of Lake Superior, Lake Michigan-Huron and Lake Erie are projected to increase by +0.19, +0.44, +0.28 m, respectively due to an increase in over-lake precipitation and basin runoff compared to relatively smaller increase in lake evaporation (Kayastha et al., 2022). While there are no studies predicting future erosion rates and shoreline recession in response to the projected water level changes for the Great Lakes, several studies show that high water levels correspond with accelerated shoreline erosion,

including bluff erosion, on short time scales (e.g. Kaczmarek et al., 2016; Krueger et al., 2020). For instance, Castedo et al. (2013) simulated erosion rates to range between 0.5-1.5 m/yr in response to lake water level variations of 0.5-1 m. A more recent study by Volpano et al. (2020) on coastal bluff erosion along Western Lake Michigan's shoreline found that erosion rates increased from 0.18-0.43 m/yr between 2009 and 2014 (period with below long term average water levels) to 0.49-1.19 m/yr between 2014 and 2018 (period with above long-term average water levels).

The outlook for marine shorelines is also concerning. On average, global sea level has risen at a rate of 3-4 mm/yr in the last 20 years (Yi et al., 2015). Future projections estimate sea level rise from 0.1-0.2 m by 2050 and from 0.3-2 m by 2100 due to ocean warming and land-based ice melt (Kopp et al., 2014; Vitousek et al., 2017). While shoreline recession is generally the combined result of various contributing factors and may be complicated by local and regional differences, it is widely acknowledged that increasing sea levels will promote shoreline recession (e.g. Anderson et al., 2015; Bruun, 1962; Dean and Houston, 2016). For instance, a recent study predicted that 15% of world's sandy beaches could face severe coastal erosion by 2050 and up to 50% by the end of the century (Vousdoukas et al., 2020). Taking into consideration the projected sea level changes and associated shoreline recession, together with the findings of our study, there is high potential that future shoreline recession will modify inputs of groundwater pollutants to coastal waters.

While this study focuses on the wastewater plume from one septic system, there are 1.2 and 1.3 million septic systems in Ontario, Canada (DeRabbie, 2020) and Michigan, United States (Department of Environment, Great Lakes and Energy, 2022), respectively, with many of these septic systems located in close proximity to the shorelines of the Great Lake.

It is also important to note that in addition to nutrients, septic-derived wastewater effluent also contains other pollutants of concern including pharmaceuticals, personal care products and pathogens, all of which may pose a risk to coastal water pollution with associated human health and ecosystem impacts. Further, many other groundwater contaminant sources are often located in coastal areas whereby shoreline recession may modify and potentially accelerate pollutant inputs to coastal waters. This includes landfills (both historic and currently operating) (Brand et al., 2018; Stefania et al., 2019) as well as industrial sites including Superfund sites which are the most contaminated sites in the United States (Carter, 2020).

4 Conclusions

This study showed the impact of shoreline recession in modifying the fate of groundwater pollutants discharging to coastal waters at a specific study site, and discussed the broader potential implications for inland and marine coastal waters. The study findings show that the shoreline recession may accelerate the discharge of groundwater pollutants to coastal waters by decreasing the subsurface travel distance and travel time. In addition, shoreline recession may modify reactive processes close to the sediment-water interface, which may in turn affect the fate of reactive pollutants and their discharge to coastal waters. Importantly, shoreline recession may result in a landward shift of the recirculation zone that commonly exists close to the shoreline, and in doing so, alter the stability and abundance of sediment phases (e.g., Fe oxides) that often act to sequester pollutants and potentially limit their release to coastal waters. In particular, the study findings show that amorphous Fe oxides may be particularly impacted by the shoreline recession and may

take time to reform and function to sequester pollutants along the modified groundwater discharge pathway.

As it is expected that climate change will accelerate shoreline recession on coastlines worldwide due to increase in the magnitude of lake water level fluctuations, sea level rise, as well as increased frequency and intensity of storm events, it is recommended that future work evaluate the impact of shoreline changes of different time scales (e.g., event based, yearly, decadal) on pollutant fate in nearshore aquifers. The nearshore aquifer at the study site was relatively homogeneous and predominantly oxidizing and it is recommended that future studies evaluate the impact of shoreline recession in different nearshore aquifer types including more heterogeneous aquifers and those with more reducing conditions. Further, while this study focused on a freshwater coastal aquifer, field investigations are required to determine the impact of shoreline recession on the functioning of the reaction zone in nearshore aquifers along marine shorelines (i.e., subterranean estuary) and the corresponding impact on pollutant fluxes to marine waters. As the study data also demonstrate that the abundance and form of solid phase Fe near the shoreline may vary in response to shoreline change, there is a need to better understand the mineralization process for Fe oxides to better predict the impact of future changes on their functioning especially with respect to sequestering and releasing pollutants of concern. While this study focused on the impact of shoreline recession on nutrients derived from a septic system, it is recommended that future studies explore the potential impacts of shoreline recession on the discharge of other anthropogenic pollutants of concern that are commonly elevated in coastal groundwater systems.

Acknowledgements

This research was supported by a Natural Sciences and Engineering Research Council of Canada (NSERC) CREATE Grant (449311-2014), NSERC Strategic Grant (STPGP 430698-12) and NSERC Discovery Grant (03686-2015).

References

Adams, K.D., Minor, T.B., 2002. Historic shoreline change at Lake Tahoe from 1938 to 1998 and its impact on sediment and nutrient loading. J. Coast. Res. 18, 637–651.

Akinbola, G.E., Adigun, M.O., Aduroja, O., 2013. Dithionite and oxalate extraction of iron and manganese in some basement complex soils of southwestern Nigeria. J. Exp. Sci. 4, 22–26

Anderson, T.R., Fletcher, C.H., Barbee, M.M., Frazer, L.N., Romine, B.M., 2015. Doubling of coastal erosion under rising sea level by mid-century in Hawaii. Nat. Hazards 78, 75–103. https://doi.org/10.1007/s11069-015-1698-6

Anwar, N., Robinson, C., Barry, D.A., 2014. Influence of tides and waves on the fate of nutrients in a nearshore aquifer: Numerical simulations. Adv. Water Resour. 73, 203–213. https://doi.org/10.1016/j.advwatres.2014.08.015

Argyilan, E.P., Forman, S.L., 2003. Lake level response to seasonal climatic variability in the Lake Michigan-Huron system from 1920 to 1995. J. Great Lakes Res. 29, 488–500. https://doi.org/10.1016/S0380-1330(03)70453-5

Beck, A.J., Kellum, A.A., Luek, J.L., Cochran, M.A., 2016. Chemical flux associated with spatially and temporally variable submarine groundwater discharge, and chemical modification in the subterranean estuary at Gloucester Point, VA (USA). Estuaries and Coasts 39, 1–12. https://doi.org/10.1007/s12237-015-9972-0

Beck, M., Dellwig, O., Schnetger, B., Brumsack, H.J., 2008. Cycling of trace metals (Mn, Fe, Mo, U, V, Cr) in deep pore waters of intertidal flat sediments. Geochim. Cosmochim. Acta 72, 2822–2840. https://doi.org/10.1016/j.gca.2008.04.013

Bełdowska, M., Bełdowski, J., Kwasigroch, U., Szubska, M., Jędruch, A., 2022. Coastal cliff erosion as a source of toxic, essential and nonessential metals in the marine environment. Oceanologia. https://doi.org/10.1016/j.oceano.2022.04.001

Bird, E.C.., 2008. Coastal geomorphology, Second Edition. John Wiley & Sons Ltd. West Sussexx. England.

Brand, J.H., Spencer, K.L., O'shea, F.T., Lindsay, J.E., 2018. Potential pollution risks of historic landfills on low-lying coasts and estuaries. WIREs Water 5, 1–12. https://doi.org/10.1002/wat2.1264

Braun, K.N., Theuerkauf, E.J., Masterson, A.L., Curry, B.B., Horton, D.E., 2019. Modeling organic carbon loss from a rapidly eroding freshwater coastal wetland. Sci. Rep. 9, 1–13. https://doi.org/10.1038/s41598-019-40855-5

Brooks, S.M., Spencer, T., Christie, E.K., 2017. Storm impacts and shoreline recovery: Mechanisms and controls in the southern North Sea. Geomorphology 283, 48–60. https://doi.org/10.1016/j.geomorph.2017.01.007

Bruun, P., 1962. Sea-level rise as a cause of shore erosion. J. Waterw. Harb. Div. 88. https://doi.org/10.1061/JWHEAU.0000252

Burningham, H., French, J., 2017. Understanding coastal change using shoreline trend analysis supported by cluster-based segmentation. Geomorphology 282, 131–149. https://doi.org/10.1016/j.geomorph.2016.12.029

Canadian Council of Ministers of the Environment, 2014. Canadian Water Quality Guidelines for the Protection of Aquatic Life.

Carter, Jacob, Casey Kalman. 2020. A toxic relationship: Extreme coastal flooding and Superfund sites. Cambridge, MA: Union of Concerned Scientists. https://www.ucsusa.org/resources/toxic-relationship

Castedo, R., Fernández, M., Trenhaile, A.S., Paredes, C., 2013. Modeling cyclic recession of cohesive clay coasts: Effects of wave erosion and bluff stability. Mar. Geol. 335, 162–176. https://doi.org/10.1016/j.margeo.2012.11.001

Charette, M.A., Sholkovitz, E.R., 2002. Oxidative precipitation of groundwater-derived ferrous iron in the subterranean estuary of a coastal bay. Geophys. Res. Lett. 29, 85-1-85–4. https://doi.org/10.1029/2001gl014512

Davidson, M.A., Turner, I.L., Splinter, K.D., Harley, M.D., 2017. Annual prediction of shoreline erosion and subsequent recovery. Coast. Eng. 130, 14–25. https://doi.org/10.1016/j.coastaleng.2017.09.008

Dean, R.G., Houston, J.R., 2016. Determining shoreline response to sea level rise. Coast. Eng. 114, 1–8. https://doi.org/10.1016/j.coastaleng.2016.03.009

Dean, W.E., Neff, B.P., Rosenberry, D.O., Winter, T.C., Parkhurst, R., 2003. The significance of groundwater to the accumulation of iron and manganese in the sediments of two hydrologically distinct lakes in North-Central Minnesota: a geological perspective. GroundWater 41, 951–963. https://doi.org/10.1111/j.1745-6584.2003.tb02437.x

Department of Environment, Great Lakes and Energy, 2022. Septic Smart

https://www.michigan.gov/egle/about/organization/drinking-water-and-environmental-health/onsite-wastewater-management/septicsmart

Department of Fisheries and Oceans Canada Buoy, 2014. C45149 Southern Lake Huron http://www.meds-sdmm.dfo-mpo.gc.ca/isdm-gdsi/waves-vagues/data-donnees/index-eng.asp

DeRabbie, D., 2020. Septic Systems and Homeowner Insurance. Ontario Onsite Wastewater Association Newsletter, 15, 1. https://www.oowa.org/wp-content/uploads/2020/05/R_Vol15_Iss1.pdf

Destouni, G., Persson, K., Prieto, C., Jarsjö, J., 2010. General quantification of catchment-scale nutrient and pollutant transport through the subsurface to surface and coastal waters. Environ. Sci. Technol. 44, 2048–2055. https://doi.org/10.1021/es902338y

Eyles, N., Meulendyk, T., 2012. Ground-penetrating radar stratigraphy and depositional model for evolving Late Holocene aeolian dunes on the Lake Huron coast, Ontario. J. Great Lakes Res. 38, 708–719. https://doi.org/10.1016/j.jglr.2012.09.003

Fuller, C.C., Dadis, J.A., Waychunas, G.A., 1993. Surface chemistry of ferrihydrite: Part 2. Kinetics of arsenate adsorption and coprecipitation. Geochim. Cosmochim. Acta 57, 2271–2282. https://doi.org/10.1016/0016-7037(93)90568-H

García-Rubio, G., Huntley, D., Russell, P., 2015. Evaluating shoreline identification using optical satellite images. Mar. Geol. 359, 96–105. https://doi.org/10.1016/j.margeo.2014.11.002

Government of Canada - Environment and Climate Change Canada, U.S. EPA, 2009. Nearshore areas of the Great Lakes. https://doi.org/978-1-100-13563-2

Gronewold, A.D., Do, H.X., Mei, Y., Stow, C.A., 2021. A tug-of-war within the hydrologic

cycle of a continental freshwater basin. Geophys. Res. Lett. 48, 1–8. https://doi.org/10.1029/2020GL090374

Gronewold, A.D., Rood, R.B., 2019. Recent water level changes across Earth's largest lake system and implications for future variability. J. Great Lakes Res. 45, 1–3. https://doi.org/10.1016/j.jglr.2018.10.012

Gronewold, A.D., Stow, C.A., 2014. Water loss from the Great Lakes. Science (80-.). 343, 1084–1085. https://doi.org/10.1126/science.1249978

Hagenaars, G., de Vries, S., Luijendijk, A.P., de Boer, W.P., Reniers, A.J.H.M., 2018. On the accuracy of automated shoreline detection derived from satellite imagery: A case study of the sand motor mega-scale nourishment. Coast. Eng. 133, 113–125. https://doi.org/10.1016/j.coastaleng.2017.12.011

Hewlett, C., North, R.L., Johansson, J., Vandergucht, D.M., Hudson, J.J., 2015. Contribution of shoreline erosion to nutrient loading of the Lake Diefenbaker reservoir, Saskatchewan, Canada. J. Great Lakes Res. 41, 110–117. https://doi.org/10.1016/j.jglr.2014.11.020

Howard, K.W.F., Livingstone, S., 2000. Transport of urban contaminants into Lake Ontario via sub-surface flow. Urban Water 2, 183–195.

https://doi.org/10.1016/S1462-0758(00)00058-3

Kaczmarek, H., Mazaeva, O.A., Kozyreva, E.A., Babicheva, V.A., Tyszkowski, S., Rybchenko, A.A., Brykała, D., Bartczak, A., Słowiński, M., 2016. Impact of large water level fluctuations on geomorphological processes and their interactions in the shore zone of a dam reservoir. J. Great Lakes Res. 42, 926–941. https://doi.org/10.1016/j.jglr.2016.07.024

Kayastha, M.B., Ye, X., Huang, C., Xue, P., 2022. Future rise of the Great Lakes water levels under climate change. J. Hydrol. 612, 128205. https://doi.org/10.1016/j.jhydrol.2022.128205

Kopp, R.E., Horton, R.M., Little, C.M., Mitrovica, J.X., Oppenheimer, M., Rasmussen, D.J., Strauss, B.H., Tebaldi, C., 2014. Probabilistic 21st and 22nd century sea-level projections at a global network of tide-gauge sites. Earth's Futur. 2, 383–406. https://doi.org/10.1002/2014ef000239

Krueger, R., Zoet, L.K., Rawling, J.E., 2020. Coastal Bluff Evolution in Response to a Rapid Rise in Surface Water Level. J. Geophys. Res. Earth Surf. 125, 1–16. https://doi.org/10.1029/2019JF005428

Lee, J., Robinson, C., Couture, R.M., 2014. Effect of groundwater-lake interactions on arsenic enrichment in freshwater beach aquifers. Environ. Sci. Technol. 48, 10174–10181. https://doi.org/10.1021/es5020136

Lewandowski, J., Meinikmann, K., Nuetzmann, G., Rosenberry, D.O., 2015. Groundwater - the disregarded component in lake water and nutrient budgets. Part 2: Effects of groundwater on nutrients. Hydrol. Process. 29, 2922–2955. https://doi.org/10.1002/hyp.10384

Linkhorst, A., Dittmar, T., Waska, H., 2017. Molecular Fractionation of Dissolved Organic Matter in a Shallow Subterranean Estuary: The Role of the Iron Curtain. Environ. Sci. Technol. 51, 1312–1320. https://doi.org/10.1021/acs.est.6b03608

Luijendijk, A., Hagenaars, G., Ranasinghe, R., Baart, F., Donchyts, G., Aarninkhof, S., 2018. The State of the World's Beaches. Sci. Rep. 8, 1–11. https://doi.org/10.1038/s41598-018-24630-6

Malott, S., O'Carroll, D.M., Robinson, C.E., 2016. Dynamic groundwater flows and geochemistry in a sandy nearshore aquifer over a wave event. Water Resour. Res. 52, 5248–5264. https://doi.org/10.1002/2014WR015716

McAllister, S.M., Barnett, J.M., Heiss, J.W., Findlay, A.J., MacDonald, D.J., Dow, C.L., Luther, G.W., Michael, H.A., Chan, C.S., 2015. Dynamic hydrologic and biogeochemical processes drive microbially enhanced iron and sulfur cycling within the intertidal mixing zone of a beach aquifer. Limnol. Oceanogr. 60, 329–345. https://doi.org/10.1111/lno.10029

McKeague, J.A., Day, J.H., 1966. Dithionite and oxalate extractable Fe and Al as aids in differentiating various classes of soild. Can. J. Soil Sci. 46, 13–22. https://doi.org/10.4141/cjss66-003

Mehra, O.P., 1958. Iron oxide removal from soils and clays by a dithionite-citrate system buffered with sodium bicarbonate. Clays Clay Miner. 7, 317–327. https://doi.org/10.1346/ccmn.1958.0070122

Meile, C., Porubsky, W.P., Walker, R.L., Payne, K., 2010. Natural attenuation of nitrogen loading from septic effluents: Spatial and environmental controls. Water Res. 44, 1399–1408. https://doi.org/10.1016/j.watres.2009.11.019

Mitchell, M., Isdell, R.E., Herman, J., Tombleson, C., 2021. Impact Assessment and Management Challenges of Key Rural Human Health Infrastructure Under Sea Level Rise. Front. Mar. Sci. 8, 1–8. https://doi.org/10.3389/fmars.2021.631757

Moore, W.S., 2010. The effect of submarine groundwater discharge on the ocean. Ann. Rev. Mar. Sci. 2, 59–88. https://doi.org/10.1146/annurev-marine-120308-081019

Mukhopadhyay, A., Ghosh, P., Chanda, A., Ghosh, A., Ghosh, S., Das, S., Ghosh, T., Hazra, S., 2018. Threats to coastal communities of Mahanadi delta due to imminent consequences of erosion – Present and near future. Sci. Total Environ. 637–638, 717–729. https://doi.org/10.1016/j.scitotenv.2018.05.076

Nielsen, P., 2009. Coastal and Estuarine Processes. World Scientific, Singapore. https://doi.org/10.1142/7114

Nisbeth, C.S., Jessen, S., Bennike, O., Kidmose, J., Reitzel, K., 2019. Role of groundwater-borne geogenic phosphorus for the internal P release in shallow lakes. Water (Switzerland) 11, 1–16. https://doi.org/10.3390/w11091783

Niswonger, R.G., Panday, S., Motomu, I., 2011. MODFLOW-NWT , A Newton formulation for MODFLOW-2005. USGS reports 44.

Rakhimbekova, S., O'Carroll, D.M., Andersen, M.S., Wu, M.Z., Robinson, C.E., 2018. Effect of transient wave forcing on the behavior of arsenic in a nearshore aquifer. Environ. Sci. Technol. 52, 12338–12348. https://doi.org/10.1021/acs.est.8b03659

Rakhimbekova, S., O'Carroll, D.M., Oldfield, L.E., Ptacek, C.J., Robinson, C.E., 2021a. Spatiotemporal controls on septic system derived nutrients in a nearshore aquifer and their discharge to a large lake. Sci. Total Environ. 752. https://doi.org/10.1016/j.scitotenv.2020.141262

Rakhimbekova, S., O'Carroll, D.M., Robinson, C.E., 2021b. Factors controlling phosphorus mobility in nearshore aquifers adjacent to large lakes. Sci. Total Environ. 799, 149443. https://doi.org/10.1016/j.scitotenv.2021.149443

Rakhimbekova, S., O'Carroll, D.M., Robinson, C.E., 2021c. Occurrence of arsenic in nearshore aquifers adjacent to large inland lakes. Environ. Sci. Technol. https://doi.org/10.1021/acs.est.1c02326

Robinson, C., 2015. Review on groundwater as a source of nutrients to the Great Lakes and their tributaries. J. Great Lakes Res. 41, 941–950. https://doi.org/10.1016/j.jglr.2015.08.001

Robinson, C.E., Xin, P., Santos, I.R., Charette, M.A., Li, L., Barry, D.A., 2018. Groundwater dynamics in subterranean estuaries of coastal unconfined aquifers: Controls on submarine groundwater discharge and chemical inputs to the ocean. Adv. Water Resour. 115, 315–331. https://doi.org/10.1016/j.advwatres.2017.10.041

Rosenberry, D.O., Lewandowski, J., Meinikmann, K., Nützmann, G., 2015. Groundwater - the disregarded component in lake water and nutrient budgets . Part 1 : effects of groundwater on hydrology. Hydrol. Process. 2921, 2895–2921. https://doi.org/10.1002/hyp.10403

Roy, J.W., 2019. Endobenthic organisms exposed to chronically high chloride from groundwater discharging along freshwater urban streams and lakeshores. Environ. Sci. Technol. 53, 9389–9397. https://doi.org/10.1021/acs.est.9b02288

Roy, J.W., Malenica, A., 2013. Nutrients and toxic contaminants in shallow groundwater along Lake Simcoe urban shorelines. Inl. Waters. https://doi.org/10.5268/IW-3.2.521

Schwertmann, U., 1964. Differenzierung der eisenoxide des bodens durch extraktion mit ammonium-losung. https://doi.org/10.1002/jpln.3591050303

Sellinger, C.E., Stow, C.A., Lamon, E.C., Qian, S.S., 2008. Recent water level declines in the Lake Michigan-Huron system. Environ. Sci. Technol. 42, 367–373.

https://doi.org/10.1021/es070664+

Sirois, M., Couturier, M., Barber, A., Gélinas, Y., Chaillou, G., 2018. Interactions between iron and organic carbon in a sandy beach subterranean estuary. Mar. Chem. 202, 86–96. https://doi.org/10.1016/j.marchem.2018.02.004

Small, C., Nicholls, R.J., 2003. A global analysis of human settlement in coastal zones. J. Coast. Res. 19, 584–599.

Spiteri, C., Regnier, P., Slomp, C.P., Charette, M.A., 2006. pH-Dependent iron oxide precipitation in a subterranean estuary. J. Geochemical Explor. 88, 399–403. https://doi.org/10.1016/j.gexplo.2005.08.084

Spiteri, C., Slomp, C.P., Charette, M.A., Tuncay, K., Meile, C., 2008. Flow and nutrient dynamics in a subterranean estuary (Waquoit Bay, MA, USA): Field data and reactive transport modeling. Geochim. Cosmochim. Acta 72, 3398–3412. https://doi.org/10.1016/j.gca.2008.04.027

Stefania, G.A., Rotiroti, M., Buerge, I.J., Zanotti, C., Nava, V., Leoni, B., Fumagalli, L., Bonomi, T., 2019. Identification of groundwater pollution sources in a landfill site using artificial sweeteners, multivariate analysis and transport modeling. Waste Manag. 95, 116–128. https://doi.org/10.1016/j.wasman.2019.06.010

Swenson, M.J., Wu, C.H., Edil, T.B., Mickelson, D.M., 2006. Bluff recession rates and wave impact along the Wisconsin coast of Lake Superior. J. Great Lakes Res. 32, 512–530. https://doi.org/10.3394/0380-1330(2006)32[512:BRRAWI]2.0.CO;2

Theuerkauf, E.J., Braun, K.N., Nelson, D.M., Kaplan, M., Vivirito, S., Williams, J.D., 2019.

Coastal geomorphic response to seasonal water-level rise in the Laurentian Great Lakes: An example from Illinois Beach State Park, USA. J. Great Lakes Res. 45, 1055–1068. https://doi.org/10.1016/j.jglr.2019.09.012

US EPA, 1996. Method 3050B Acid digestion of sediments, sludges and soils, Method 3050B Acid digestion of sediments, sludges and soils.

Vitousek, S., Barnar, P.L., Fletcher, C.H., Frazer, N., Storlazzi, C.D., 2017. Doubling of coastal flooding frequency within decades due to sea-level rise 1–9. https://doi.org/10.1038/s41598-017-01362-7

Vogel, L.J., O'Carroll, D.M., Edge, T.A., Robinson, C.E., 2016. Release of Escherichia coli from Foreshore Sand and Pore Water during Intensified Wave Conditions at a Recreational Beach. Environ. Sci. Technol. 50, 5676–5684. https://doi.org/10.1021/acs.est.6b00707

Vousdoukas, M.I., Ranasinghe, R., Mentaschi, L., Plomaritis, T.A., Athanasiou, P., Luijendijk, A., Feyen, L., 2020. Sandy coastlines under threat of erosion. Nat. Clim. Chang. 10, 260–263. https://doi.org/10.1038/s41558-020-0697-0

Yi, S., Sun, W., Heki, K., Qian, A., 2015. An increase in the rate of global mean sea level rise since 2010. Geophys. Res. Lett. 42, 3998–4006. https://doi.org/10.1002/2015GL063902

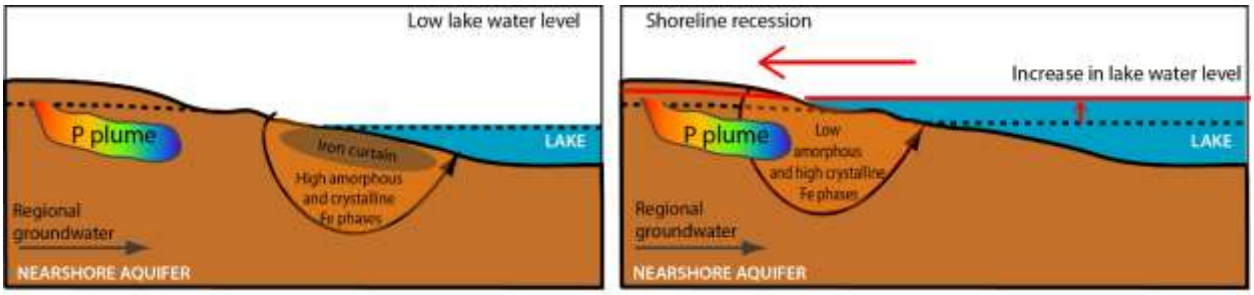

Abstract Art

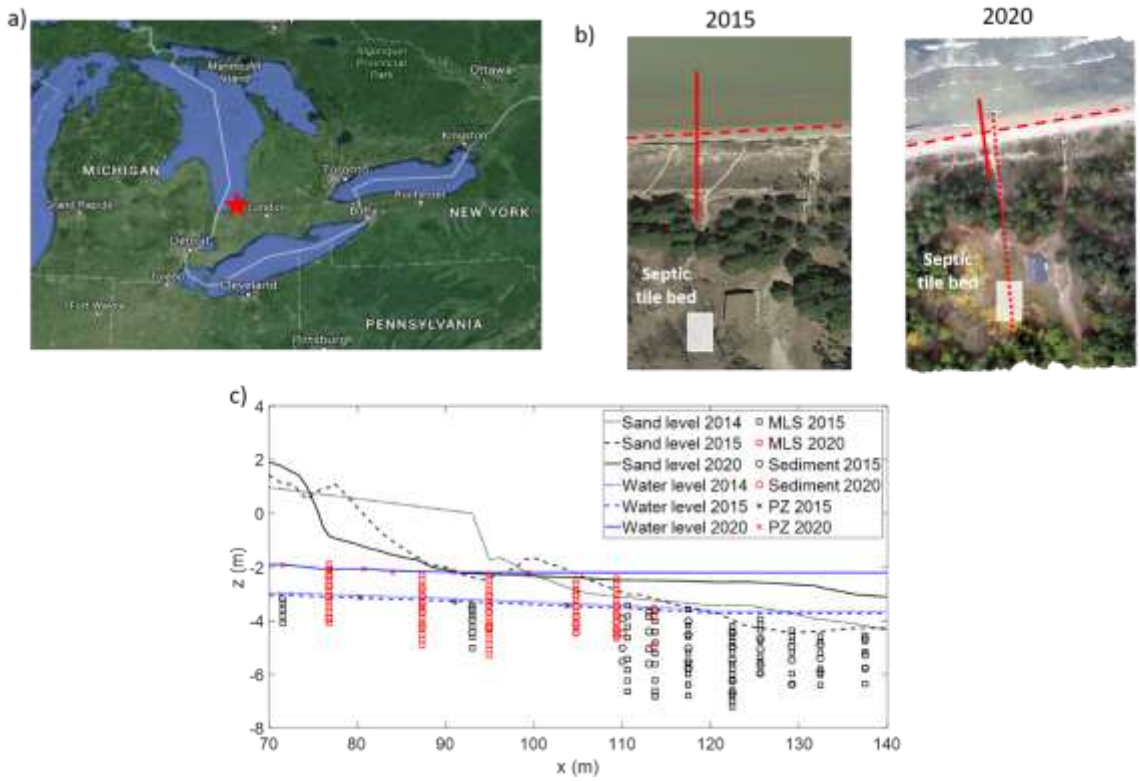

Figure 1. a) Map of Laurentian Great Lakes Basin with the red star indicating the location of the study site. b) Aerial image of the study site using Google Earth imagery in 2015 and Drone (DJI Mavic Air) image in 2020, red dashed lines indicate the shoreline location in each image, solid red lines indicate the cross-shore monitoring transect location, and red dotted line indicates the ERT survey line. The location of septic tile bed is marked with a white rectangle. c) Layout of monitoring equipment along the cross-shore transect for sampling events in 2014 and 2015, and in 2020. Sand and water levels measured in 2014, 2015 and 2020 are also shown in (c).

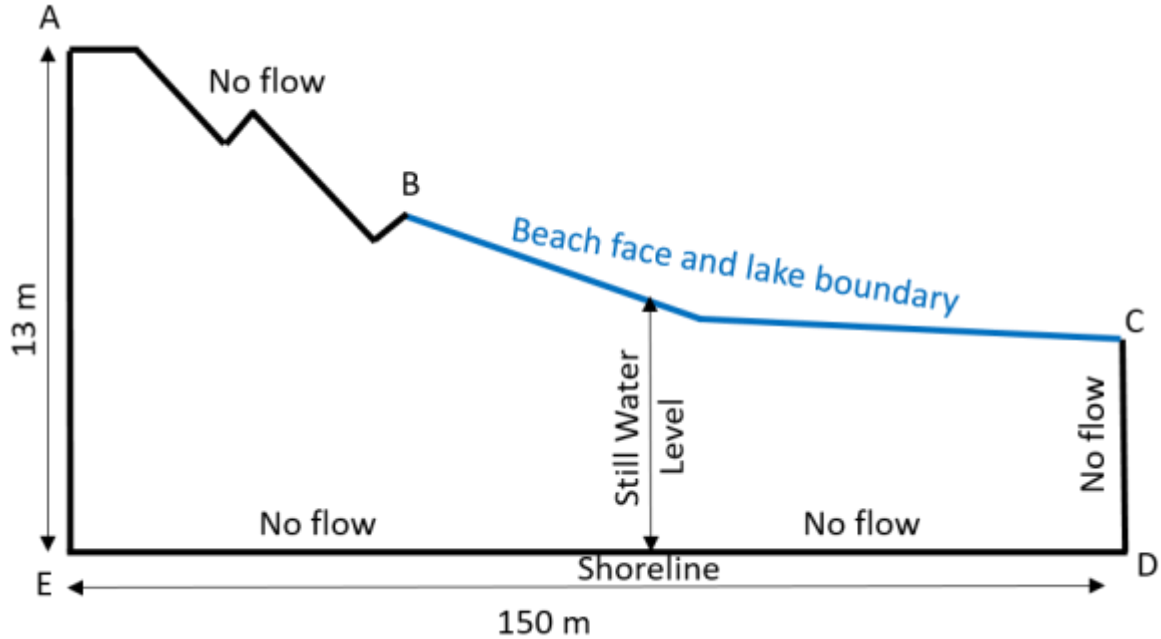

Figure 2. Numerical groundwater model domain including flow boundary conditions.

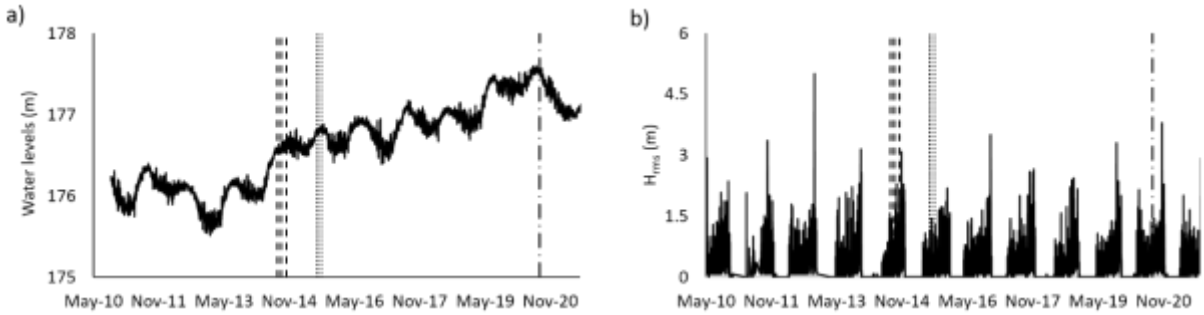

Figure 3. a) Average daily lake water levels measured at offshore buoy located 70 km north of the study site (Lake Huron at Goderich (02FE012) with elevation based on International Great Lakes Datum 1985 (Fisheries and Oceans Canada, 2020). b) Offshore root mean square wave height (H_{rms}) measured at a buoy (C45149 Southern Lake H) located ~35 km offshore from the field site. The vertical black dashed lines in a) and b) indicate days of field sampling events.

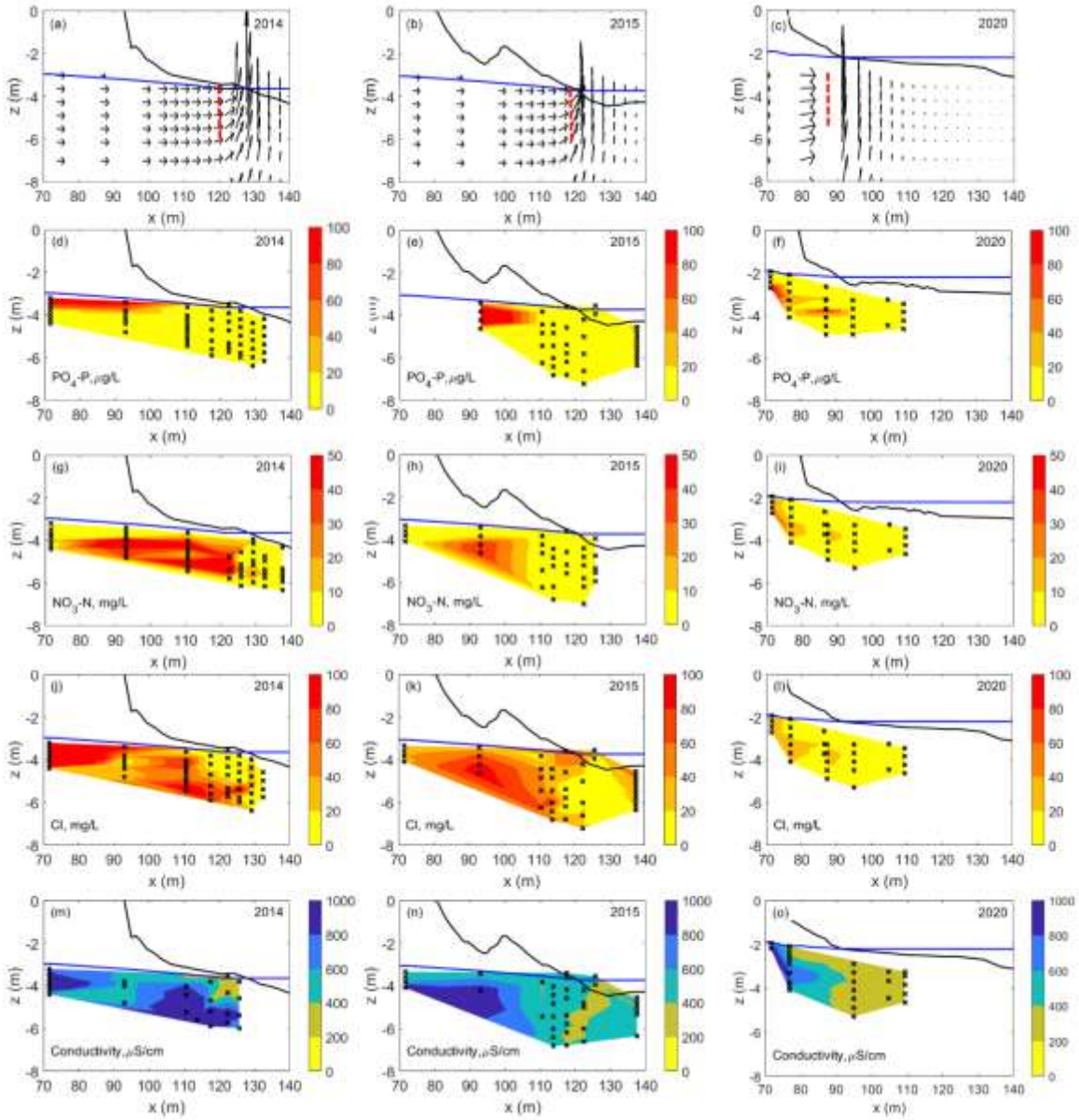

Figure 4. Simulated groundwater flow velocities based on the hydrological conditions during the a) 2014, b) 2015, and c) 2020 sampling periods. Distribution of d-f) PO_4-P, g-i) NO_3-N, j-l) chloride (Cl) and m-o) electrical conductivity (EC) in 2014, 2015 and 2020. For all subplots, the solid blank line represents the sand surface elevation and the solid blue line represents the measured water levels for each sampling event. Red dashed lines in a-c) indicate lines across which PO_4-P and NO_3-N fluxes were calculated using the simulated groundwater fluxes and interpolated PO_4-P and NO_3-N concentrations (x = 120.3 m in 2014 and 2015 and x = 88.7 in 2020). Colored contours in d-o) represent the concentrations of PO_4-P, NO_3-N, Cl and EC with the color bars shown on the right hand side, and black crosses show pore water sampling locations.

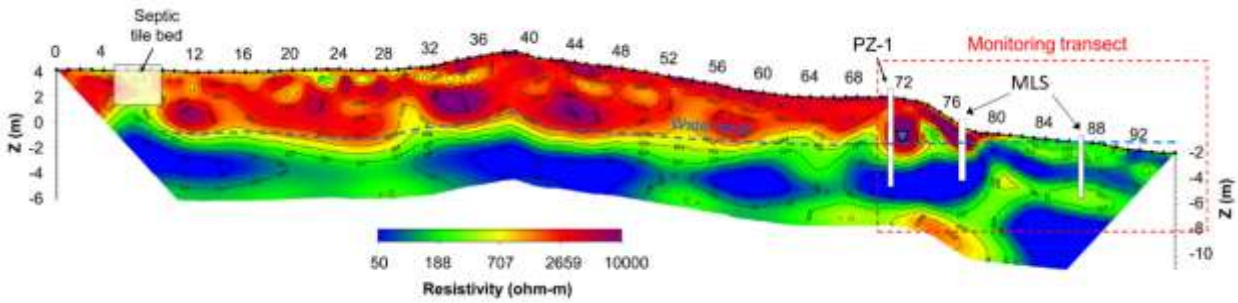

Figure 5. Cross-sectional resistivity image from the ERT survey. The septic drainage field, PZ-1 and MLS are indicated, along with the inferred water table (blue dashed line). The extent of the cross-shore monitoring transect is defined by the red dashed box.

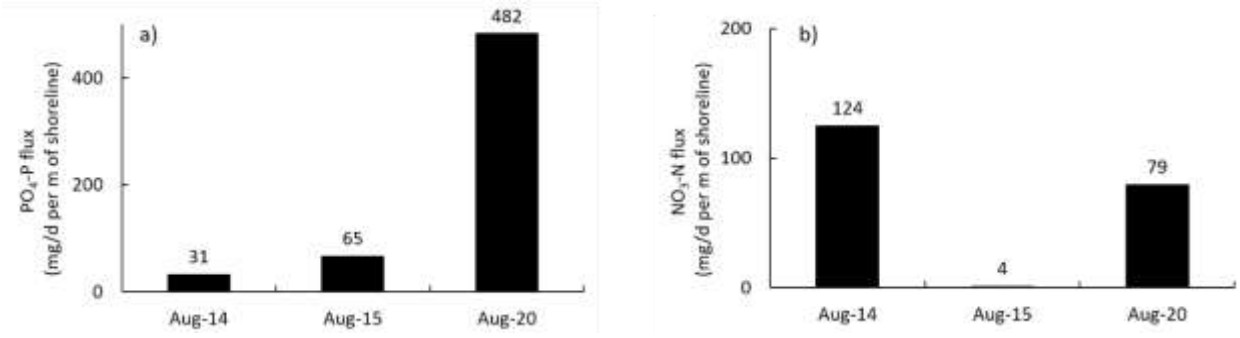

Figure 6. Estimated a) PO_4-P and b) NO_3-N flux directed towards the sediment-water interface for August 2014, 2015 and 2020 sampling events.

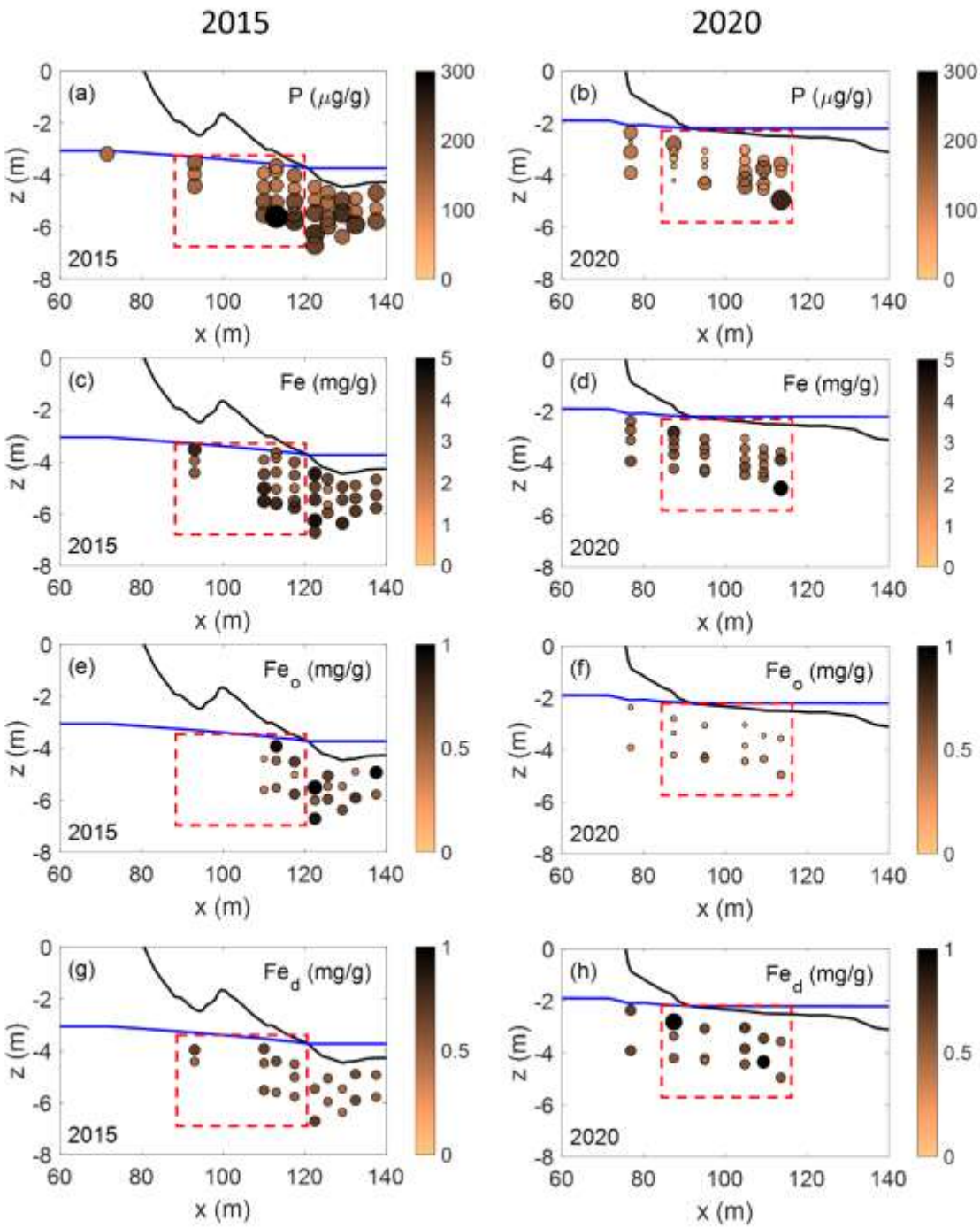

Figure 7. Distribution of a, e) solid-phase P, b, f) solid phase Fe, c, g) oxalate-extractable, amorphous Fe phases and d, h) dithionite-extractable, more crystalline Fe phases in 2015 and 2020. Rows show the year of sampling event when sediment sample was collected and columns show the different P and Fe solid phase extraction data. The bubble sizes and color bar indicate the magnitude of the solid-phase concentration. The solid black line represents the sand surface elevation, and the solid blue line represents the measured water levels at each site. Only the samples within the red box were considered in comparing the abundance of solid-phase P and Fe between sampling years.

Supporting Information

Potential for shoreline recession to accelerate pollutant fluxes across the groundwater-coastal water interface

Sabina Rakhimbekova[a*], Christopher Power[a], Denis M. O'Carroll[b], Clare E. Robinson[a]

[a] Department of Civil and Environmental Engineering, Western University, London ON, N6A 5B9, Canada.

Email: srakhimb@uwo.ca

[b] School of Civil and Environmental Engineering, Water Research Centre, University of New South Wales, Manly Vale NSW 2093, Australia.

*corresponding author: Dr. Sabina Rakhimbekova

7 pages

Contents **Page**

S1. Sediment extraction methods

Ammonium oxalate and sodium dithionite sediment extractions were conducted on select sediments samples collected in 2015 and 2020 to characterize different Fe-bearing solid phase pools. For the sodium dithionite extraction, 4 g of sediment samples was placed in a 250 mL centrifuge bottle and 40 mL of 0.3 M Na-citrate solution and 5 mL of 1 M $NaHCO_3$ solution were added (Mehra, 1958). The solution was treated in a water bath at 80°C and 1 g of solid $Na_2S_2O_4$ was added to flocculate the sample, after which the solution was stirred continuously for 1 min and then occasionally for a total of 15 min. The solution was then centrifuged at 2000 rpm for 5 minutes, after which the clear supernatant was decanted, filtered and analyzed for dissolved Fe using flame atomic absorption spectroscopy (FAAS, Agilent 200 Series). For the ammonium oxalate extraction, 1 g of sediment sample was placed in a 250 mL centrifuge bottle, 40 mL of acid oxalate solution was added and then it was placed in mechanical shaker for 4 hour in the dark (McKeague and Day, 1966). The solution was then centrifuged at 2400 rpm for 10 minutes. The clear supernatant solution was then decanted, filtered and analyzed for dissolved Fe using FAAS.

S2. Numerical model set up

Wave set-up approach has been shown to represent the main effects of waves on groundwater flow dynamics while reducing computational requirements(Robinson et al., 2014; Xin et al., 2010). Using this approach, the time-varying specified heads applied along the lake boundary (BC Figure 3) were calculated using an empirical wave setup formula developed by Nielsen(Nielsen, 2009) and given as:

$$\overline{\eta} = \frac{0.4H_{rms}}{1+10\dfrac{D+\overline{\eta}}{H_{rms}}} \quad (1)$$

where η (m) is the increase in water level above the still water level due to wave setup; H_{rms} (m) is the offshore root mean square wave height obtained from the Fisheries and Ocean Canada wave buoy (Figure 2b); and D (m) is the distance from the sediment water interface to the still water level and is a function of location across the beach face. Submerged nodes along the lake boundary were assigned a hydrostatic pressure corresponding to the wave setup profile. This was implemented using a modified form of the periodic boundary condition (PBC) package(Post, 2011) to allow a time-varying moving interface to be implemented. Nodes landward of the wave setup point along the lakeward boundary were represented as a no-flow boundary.

S3. PO_4-P and NO_3-N flux calculations

A steady state groundwater flow model was used to simulate the water flux directed towards the lake. The PO_4-P and NO_3-N fluxes near the shoreline were estimated by multiplying the simulated groundwater flux across a vertical line near the shoreline by field measured PO_4-P and NO_3-N concentrations (interpolated to a depth of 3 m below beach face). This calculation was performed for the simulated groundwater flux in 2014, 2015 and 2015 and for field measured PO_4-P and NO_3-N concentrations in each of these years with the location of the vertical line at x = 120.3 m in 2014 and 2015 and x = 88.7 m in 2020. The limitation of this calculation is that it does not consider that the measured PO_4-P and NO_3-N concentrations may be modified by dilution by surface water at shallow depth below the groundwater-lake interface.

S4. Correlation between NO_3-N and Electrical Conductivity (EC).

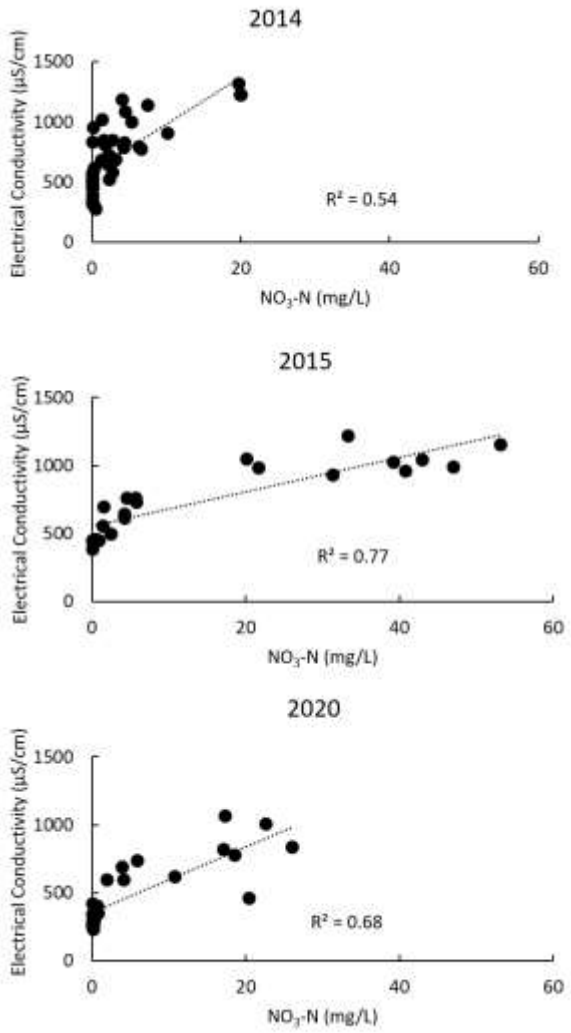

Figure S1. Correlation between NO_3-N and electrical conductivity (EC) in 2014, 2015 and 2020.

References

McKeague, J.A., Day, J.H., 1966. Dithionite and oxalate extractable Fe and Al as aids in differentiating various classes of soild. Can. J. Soil Sci. 46, 13–22. https://doi.org/10.4141/cjss66-003

Mehra, O.P., 1958. Iron oxide removal from soils and clays by a dithionite-citrate system buffered with sodium bicarbonate. Clays Clay Miner. 7, 317–327. https://doi.org/10.1346/ccmn.1958.0070122

Nielsen, P., 2009. Coastal and Estuarine Processes. World Scientific Publishing Co Pte Ltd, Singapore.

Post, V.E.A., 2011. A new package for simulating periodic boundary conditions in MODFLOW and SEAWAT. Comput. Geosci. 37, 1843–1849. https://doi.org/10.1016/j.cageo.2011.01.012

Robinson, C., Xin, P., Li, L., Barry, D.A., 2014. Groundwater flow and salt transport in a subterranean estuary driven by intensified wave conditions. Water Resour. Res. 50, 165–181. https://doi.org/10.1002/2013WR013813

Xin, P., Robinson, C., Li, L., Barry, D.A., Bakhtyar, R., 2010. Effect of wave forcing on a subterranean estuary. Water Resour. Res. 46, 1–17. https://doi.org/10.1016/j.advwatres.2006.07.006